**Naval Research Laboratory**

**Washington, DC 20375-5320**

NRL/MR/5550--97-7941

# Theoretical and Experimental Investigation of the Impedance of a Vertical Monopole over Perfect, Imperfect, and Enhanced Ground Planes

MICHAEL A. RUPAR

*Information Technology Division*

April 30, 1997

# REPORT DOCUMENTATION PAGE

*Form Approved*
*OMB No. 0704-0188*



| 1. AGENCY USE ONLY (*Leave Blank*) | 2. REPORT DATE | 3. REPORT TYPE AND DATES COVERED |
|---|---|---|
| | April 30, 1997 | Interim 1990 |

**4. TITLE AND SUBTITLE**

Theoretical and Experimental Investigation of the Impedance of a Vertical Monopole over Perfect, Imperfect, and Enhanced Ground Planes

**5. FUNDING NUMBERS**

PE: 63160D
WU: 55-3771-C-7

**6. AUTHOR(S)**

Michael A. Rupar

**7. PERFORMING ORGANIZATION NAME(S) AND ADDRESS(ES)**

Naval Research Laboratory
Washington, DC 20375-5320

**8. PERFORMING ORGANIZATION REPORT NUMBER**

NRL/MR/5550--97-7941

**9. SPONSORING/MONITORING AGENCY NAME(S) AND ADDRESS(ES)**

Office of Naval Research
Arlington, VA 22217-5660

**10. SPONSORING/MONITORING AGENCY REPORT NUMBER**

**11. SUPPLEMENTARY NOTES**

**12a. DISTRIBUTION/AVAILABILITY STATEMENT**

Approved for public release; distribution unlimited.

**12b. DISTRIBUTION CODE**

**13. ABSTRACT** (*Maximum 200 words*)

The impedance characteristics of a vertical monopole over an imperfect ground are investigated theoretically and experimentally. An expression for the change in antenna input impedance from an imperfect to a perfect ground, $\Delta Z$, is introduced, and is used to generate results which illustrate the effects of ground constants (the earth's conductivity and relative dielectric constant) on the input impedance of a vertical monopole. Calculated results are presented correlating the change in impedance to varying ground conditions and extended to the inclusion of a radial ground screen. Theoretical analysis is compared with ground constant measurements that were conducted at three locations around the Washington, DC, area. Antenna impedance measurements were performed on monopoles of various heights at one of the surveyed locations, and at the Naval Research Laboratory's Brandywine Test Facility.

**14. SUBJECT TERMS**

Impedance
Monopole
Ground constants
Conductivity
Dielectric constant
Ground screen

**15. NUMBER OF PAGES**

81

**16. PRICE CODE**

| 17. SECURITY CLASSIFICATION OF REPORT | 18. SECURITY CLASSIFICATION OF THIS PAGE | 19. SECURITY CLASSIFICATION OF ABSTRACT | 20. LIMITATION OF ABSTRACT |
|---|---|---|---|
| UNCLASSIFIED | UNCLASSIFIED | UNCLASSIFIED | UL |

NSN 7540-01-280-5500

Standard Form 298 (Rev. 2-89)
Prescribed by ANSI Std 239-18
298-102

## CONTENTS

# Theoretical and Experimental Investigation of the Impedance of a Vertical Monopole over Perfect, Imperfect, and Enhanced Ground Planes

## I. Introduction

The characteristics of vertical monopole antennas are generally well defined ([1], [2]). However, one factor that is not easily understood is the influence of the ground constants (the conductivity, $\sigma$, and relative dielectric constant, $\varepsilon_r$) on a vertical monopole's input impedance. Considering that the input impedance of a monopole less than a quarter-wavelength in height may have a resistive part less than one ohm (whereas the reactive impedance may be greater than 1000 ohms), the change in the antenna's input impedance caused by an imperfect ground can be significant.

This report examines the effects of an imperfect ground on the input impedance of a vertical monopole mounted above it, and shows that those effects are minimized through the use of a radial ground screen. A theoretical expression for the antenna impedance incorporating the ground effects is used to generate impedance values for a variety of earth conditions. Theoretical impedances are then compared with values from field measurements of monopoles. Methods of determining the ground constants for a particular site are also presented, along with results of actual area surveys. Efforts to validate the theoretical impedance results through actual antenna measurements are presented and are shown to be only partially successful.

This paper focuses on the effects on the monopole impedance due to the ground, both with and without ground systems present. The general theory is briefly presented in Section II, and is complimented by a detailed theoretical development of the monopole impedance over an imperfect ground in Appendix A. Using expressions from Section II, Section III contains explicit impedance calculations for ground conditions with characteristics similar to those found in the local (Washington, DC) area for a number of monopole heights. These calculated results are then compared to monopole impedances generated by an antenna modeling program. Section IV contains the results of measurements of monopole impedance performed at a "perfect" ground plane facility and over a normal, "imperfect", ground plane. Section V details similar experimental measurements taken when a finite ground

Manuscript approved March 10, 1997.

screen is introduced. Appendix B presents a method for measuring the ground constants for a particular area, and contains the results of ground site surveys conducted in the local area.

## II. Theory

Two factors detrimentally affect the input impedance of a short vertical monopole over an imperfect ground. These factors are the limited height of the antenna and the less than ideal conductivity of the earth beneath it. The current distribution on a short monopole results in a very large input capacitive reactance.

The earth ground causes an increase in the input resistance of a vertical monopole due to the ground currents induced by the radiated fields. This contribution in resistance can be much greater than the original radiation resistance of the monopole, resulting in a significant loss of radiated power in the ground and severely reducing the antenna efficiency. The situation can be improved by the use of a radial ground screen, which provides a low-loss return path for the antenna base current.

To develop an expression for the input impedance of a vertical monopole over an imperfect ground, one starts with a simple vertical antenna element along the z-axis of height h, situated above a ground half-space, as shown in Figure 1. Shown are the terms identifying the electrical and magnetic properties of the two half-spaces of air and earth. The terms for the earth (or ground) half-space are called the ground constants. Note that these "constants" are functions of the mineral and moisture content of the ground, and may also be a function of frequency. The magnetic permeability of the medium is $\mu$, and the permittivity is $\varepsilon$ ($\mu_o$ and $\varepsilon_o$ for free space). The third ground constant, $\sigma$, is the conductivity of the ground plane, and equals zero for the free space condition.

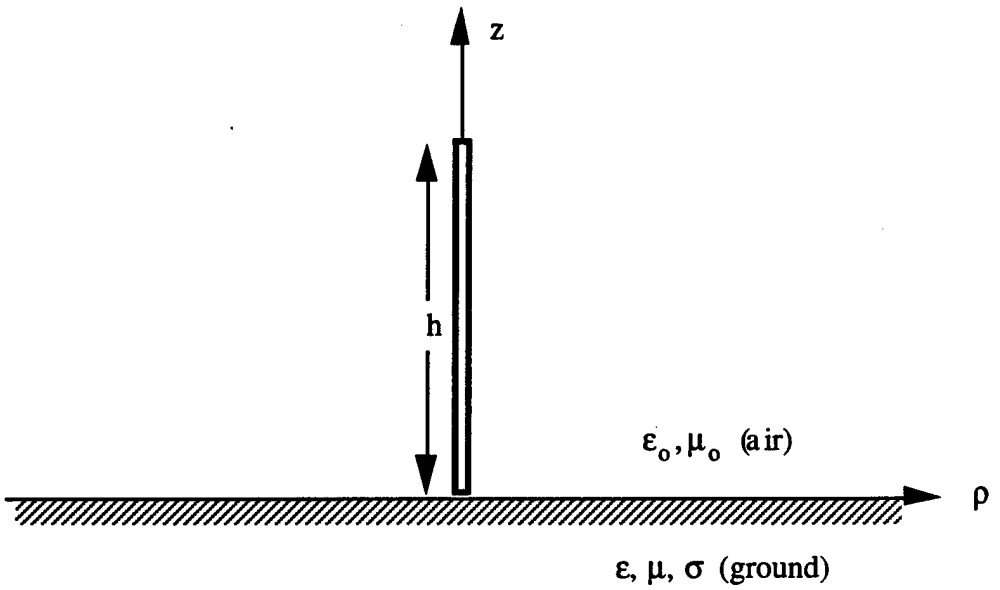


Figure 2.1: The representation of a vertical monopole over an imperfect ground. The monopole is just above the ground plane.

The propagation constant ($\gamma$) and the characteristic impedance ($\eta$) of the imperfect ground are:

$$\gamma = \sqrt{j\omega\mu(\sigma + j\omega\varepsilon)}$$

$$\eta = \sqrt{\frac{j\omega\mu}{j\omega\varepsilon + \sigma}}$$

For normal soil with little inherent magnetization, one can assume $\mu = \mu_o$. For free space, the above quantities are defined as:

$$\gamma_o = j\omega\sqrt{\mu_o\varepsilon_o} \equiv j\beta = j\,\frac{2\pi}{\lambda}$$

$$\eta_o = \sqrt{\frac{\mu_o}{\varepsilon_o}}$$

where $\lambda$ equals the wavelength of the antenna's intended frequency of operation, and $\beta$ is the free space propagation constant. The free space quantities $\gamma_o$ and $\eta_o$ are virtually identical to the those for air, and will be used for the air half-space.

The antenna's self-impedance is separated into two parts,

$$Z_T = Z_O + \Delta Z_T \qquad (2.1)$$

where $Z_T$ is the total input impedance, and $Z_O$ is the input impedance of the same antenna over a perfect ground. $\Delta Z_T$ represents the difference between the perfect and imperfect ground cases. One may think of the perfect ground case as an infinite ground screen.

$\Delta Z_T$ was defined by Wait in [3], where it was also applied to both the lossy ground and the imperfect ground screen problems. The development of $\Delta Z_T$ is detailed in Appendix A.

$\Delta Z_T$ ,written in cylindrical coordinates (where $\rho = \sqrt{x^2 + y^2}$), is expressed as:

$$\Delta Z_T \cong \eta \int_0^\infty [H_\varnothing(\rho,0)]^2 \, 2\pi\rho \, d\rho \qquad (2.2)$$

where $H_\varnothing(\rho,0)$ is the tangential magnetic field at the surface, defined below as:

$$H_\varnothing(\rho,0) = -\frac{j}{2\pi \sin\alpha} \left[ \frac{e^{-j\beta r}}{\rho} \cos(\beta h - \alpha) - \frac{e^{-j\beta\rho}}{\rho} \cos\alpha - \frac{jh}{\rho} \frac{e^{-j\beta r}}{r} \sin(\alpha - \beta h) \right] \qquad (2.3)$$

with

$r = (z^2 + \rho^2)^{1/2}$

$\alpha = \beta(h + ht)$

$\beta$ = free space propagation constant

h = height of monopole

ht = effective contribution to monopole height from top loading

For the case where there is no top loading (ht = 0), $\alpha = \beta h$, and $\Delta Z_T$ can be reduced to:

$$\Delta Z_T = \frac{-\eta}{2\pi \sin^2 \beta h} \left[ \int_0^\infty \frac{e^{-j2\beta r}}{\rho} d\rho - 2\cos\beta h \int_0^\infty \frac{e^{-j\beta(r+\rho)}}{\rho} d\rho - \cos^2 \beta h \int_0^\infty \frac{e^{-j2\beta\rho}}{\rho} d\rho \right] \quad (2.4)$$

These expressions are valid only when $|\gamma| >> \beta$, which limits one to cases where the displacement currents (changes in the electric field with respect to time, rather than free electron flow) in the ground are negligible. This condition is expressed as:

$$\left| \sqrt{j\mu\omega\sigma - \omega^2\mu\varepsilon} \right| >> \omega\sqrt{\mu_o \varepsilon_o} \quad (2.5)$$

With $\rho$ in the denominator of each term of equation (2.4), there is a singularity at $\rho = 0$. Since the object is to calculate the change in impedance from a perfect to imperfect ground, including a base plate made of a good conductor does not contribute to the expression for $\Delta Z_T$. Therefore, one can substitute the value "a" for the lower limit of $\rho$ , where "a" is the radius of the "perfect" base.

Adding a Radial Ground Screen

The inclusion of a radial ground screen at the base of the antenna has a significant effect on the impedance expression for the monopole. An antenna ground system supplies a low-resistance path from the antenna base out to a radial distance where the radial current density in the soil no longer contributes an appreciable power loss.

Although equation (2.2) still applies for the region beyond the ground screen ($\rho > b$), a separate expression is necessary to account for the screen's effect on the surface magnetic and electric fields. The vertical monopole with a radial ground screen is shown in Figure 2.2.

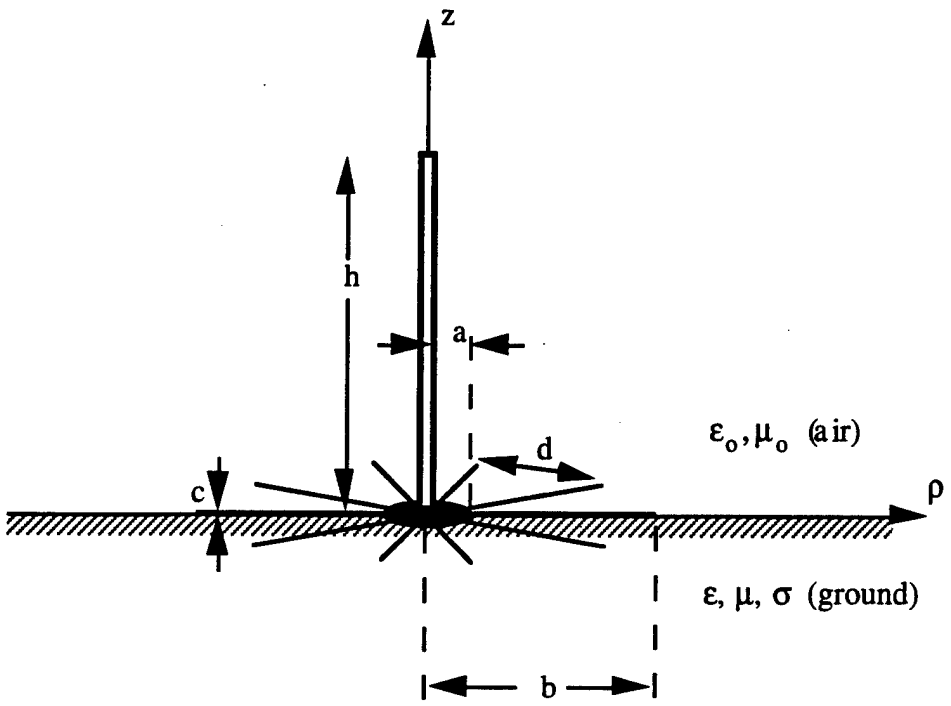


Figure 2.2: The representation of a vertical monopole with a radial ground screen of length b over an imperfect earth ground. Note that d is the linear spacing between the ends of the radial conductors.

For the region $\rho > b$, the impedance of the ground is just the characteristic impedance, $\eta$, but when the ground radials are present ($\rho < b$), the impedance is the parallel combination of the screen impedance, $\eta_e$, and the surface impedance, $\eta$. This is called the equivalent impedance, $\eta_x$ .

$$\eta_x (0 < \rho < b) = \frac{\eta \, \eta_e}{\eta + \eta_e} \tag{2.6}$$

where:

$$\eta_e = \frac{i\,\eta_o d}{\lambda} \ln \frac{d}{2\pi c}$$

$$\text{and} \quad d = \frac{2\pi\rho}{N}$$

N is the number of radials, d is the linear spacing (distance) between the ends of the radial conductors and c is the radius of the wire. This expression is an approximation, originally derived for a wire grid in free space [4], and assumes that the wires are electrically close enough to approximate a grid.

For the case of a radial ground screen, we break $\Delta Z_T$ into two parts:

$$\Delta Z_T = \Delta Z + \Delta Z_S$$

where $\Delta Z$ is the change in the input impedance of the antenna due to the influence of the imperfect ground outside the ground screen, and $\Delta Z_S$ is the change affected within the imperfect ground screen system. The two expressions for $\Delta Z_T$ are:

$$\Delta Z \cong \eta \int_b^\infty [H_\varnothing(\rho,0)]^2\, 2\pi\rho\, d\rho \qquad (2.7)$$

$$\Delta Z_S \cong \int_a^b \frac{\eta\,\eta_e}{\eta + \eta_e} [H_\varnothing(\rho,0)]^2\, 2\pi\rho\, d\rho \qquad (2.8)$$

with $H_\varnothing(\rho,0)$ remaining as defined in equation (2.3).

Equation (2.7) is identical to equation (2.2), except that the lower limit of integration is now b, representing the radius of the ground screen. Equation (2.8) differs in that the equivalent impedance term $\eta_x$ is now a function of the radial distance $\rho$, and can no longer be moved outside of the integral. The lower limit "a" still represents the radius of the conducting base plate.

To more concisely illustrate how the ground characteristics of the antenna site

affect the $\Delta Z$ calculations, the ground constants of conductivity and relative dielectric constant were combined into a single function, $\delta$. (The function $\delta$ was first introduced by Maley, et al, in [5]). The relation between the ground impedance and the constant $\delta$, referred to as the "ground factor ", is shown below:

$$\eta = \sqrt{\frac{j\,\mu\,\omega}{\sigma + j\,\omega\,\varepsilon}} = \sqrt{j}\;\eta_o\,\delta \qquad (2.9)$$

where $\delta$ is defined as:

$$\delta = \delta' \sqrt{\frac{1}{1 + j(\delta')^2 \varepsilon_r}} = |\delta|\, e^{-j\psi} \qquad (2.10)$$

with:

$$\delta' = \sqrt{\frac{\omega\,\varepsilon_o}{\sigma}}$$

$$\psi = \frac{1}{2}\tan^{-1}[(\delta')^2 \varepsilon_r]$$

with $\varepsilon_r$ being the relative dielectric constant for the ground plane. $\psi$ is referred to as the phase of the ground factor. Use of $\delta$ allows one to present calculated $\Delta Z$ results independent of a particular frequency or ground constants.

## III. Calculated Monopole Impedance Results

The theory set forth in the Section II is now used to generate a data set for predicting the performance of a vertical monopole antenna over an imperfect ground. Antenna performance is calculated using two methods. The first method uses the expressions from Section II and [3], and calculates the effect of the ground on the input impedance using Mathematica®[6], a mathematical software package. The second method is to generate a computer model of the antenna using the Numerical Electromagnetics Code (NEC) program [7] to produce values for the feedpoint impedance.

### Calculated Impedance Predictions for an Imperfect Ground

By eliminating the expression for the effects of the ground screen from the $\Delta Z_T$ expression, one can predict impedance performance of a vertical monopole over a uniform imperfect ground.

Using equation (2.4), with the limits adjusted to eliminate the singularity at $\rho$ equal to zero, (as stated in Section II), a duplication of one of the original plots in Wait's work (Figure 3 in [3]) was generated. (2.4) is written below with the corrected limits of integration for a non-singular function as equation (3.1).

$$\Delta Z_T = \frac{-\eta}{2\pi\sin^2\beta h}\left[\int_a^\infty \frac{e^{-j2\beta r}}{\rho}\,d\rho - 2\cos\beta h\int_a^\infty \frac{e^{-j\beta(r+\rho)}}{\rho}\,d\rho - \cos^2\beta h\int_a^\infty \frac{e^{-j2\beta\rho}}{\rho}\,d\rho\right] \quad (3.1)$$

where $r=\sqrt{h^2+\rho^2}$, and h is the height of the monopole.

The results, shown below, were generated using Mathematica, which (among other features) performs symbolic and numerical integration for complex expressions. Figure 3.1a shows the magnitude of the change in impedance $|\Delta Z|$ of a monopole, which is normalized with respect to the ground impedance term, $\eta$, as a function of the ground plate radius. The abscissa is the radius of the "perfect" ground upon which the antenna is centered, normalized with respect to the height of the antenna, and can be thought of as the radius of a circular perfectly conducting antenna base

plate. Computations were performed for antenna heights of 0.1λ, 0.15λ, and 0.25λ.

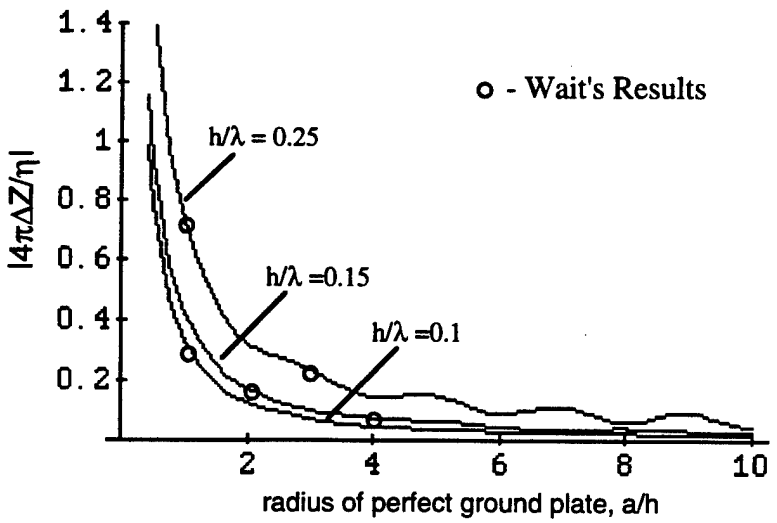


Figure 3.1a: The incremental input impedance magnitude for a vertical antenna situated over a perfectly conducting disc on a homogeneous ground, normalized with respect to the ground impedance,η.

Figure 3.1a includes values from Wait's original calculations (Figure 2 in [1]) and shows general agreement with those results. Figures 3.1b and 3.1c are similar to 3.1a, except that they illustrate the effects of the ground plate on the real and imaginary components of the normalized input impedance.

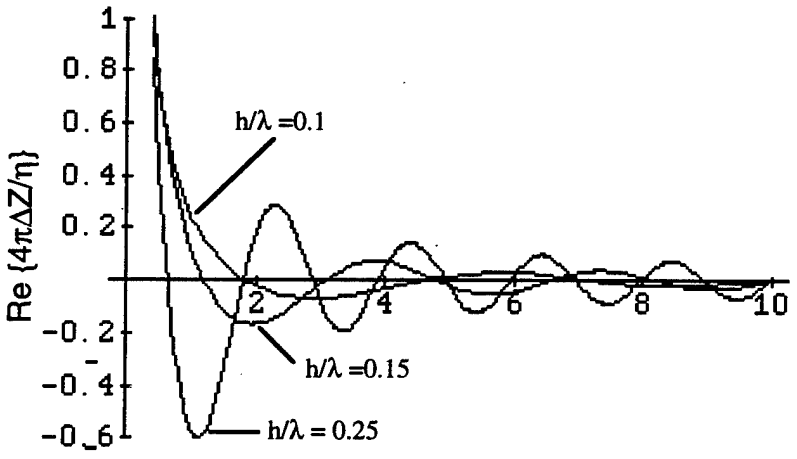


Figure 3.1b: The incremental input resistance for a vertical antenna situated over a perfectly conducting disc on a homogeneous ground, normalized with respect to the ground impedance, η.

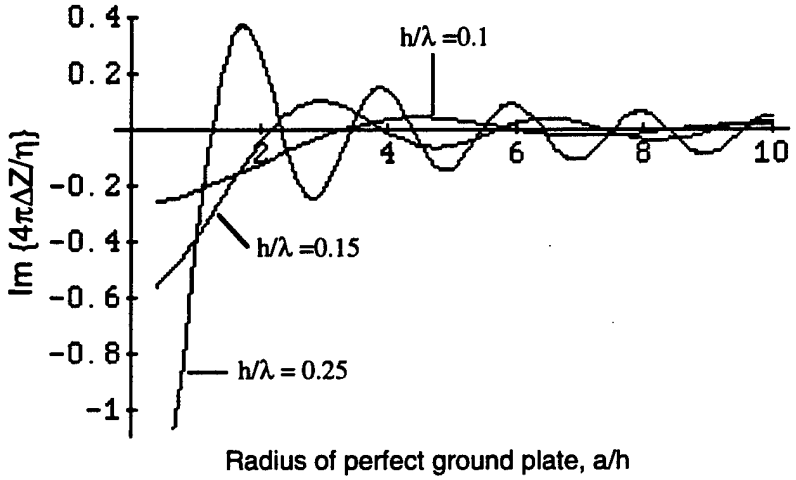


Figure 3.1c: The incremental input reactance for a vertical antenna situated over a perfectly conducting disc on a homogeneous ground, normalized with respect to the ground impedance, $\eta$.

These figures show that the greatest contributions of the ground to the antenna input impedance occur close in to the antenna. Both the area of appreciable contribution and the magnitude of the impedance change increases with the height of the monopole.

This completes the comparison with Wait's results. For the range of a/h of interest to this development, the conducting base plate (of radius a) is kept quite small compared to the height of the monopole (h). Figures 3.2a and 3.2b provide a closer examination of the normalized change in resistance and reactance for small values of a/h.

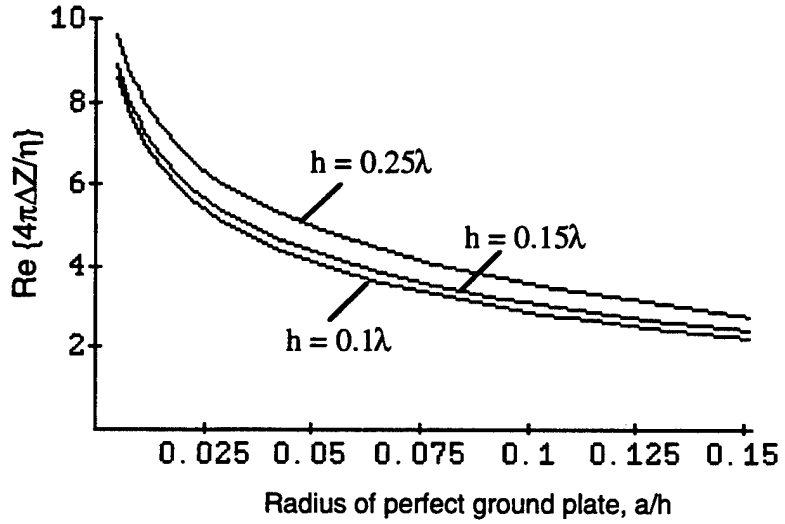


Figure 3.2a: The incremental input resistance for a vertical antenna situated over a perfectly conducting discoid on a homogeneous ground, normalized with respect to the ground impedance, $\eta$. This figure provides an illustration of the behavior of $\Delta R$ for small values of a/h.

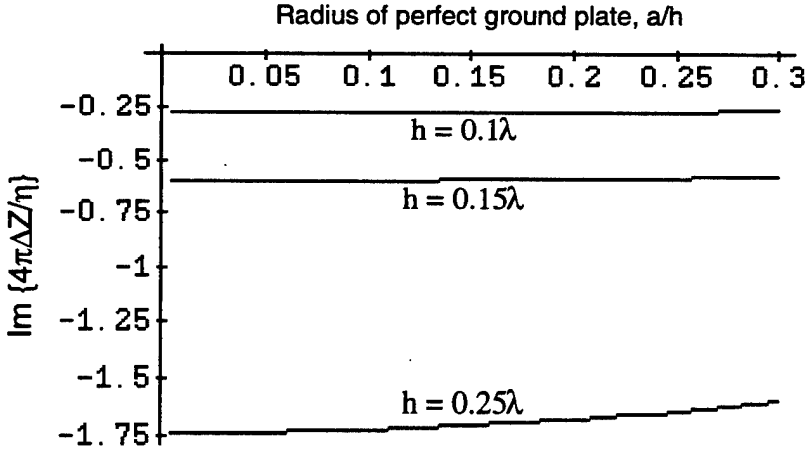


Figure 3.2b: The incremental input reactance for a vertical antenna situated over a perfectly conducting discoid on a homogeneous ground, normalized with respect to the ground impedance, $\eta$. This figure provides an illustration of the behavior of $\Delta X$ for small values of a/h.

These figures illustrate, for small values of a/h, (equivalent to having no ground plate connected to the antenna base), that $\Delta X$ is more dependant on the antenna height, while $\Delta R$ (Figure 3.2a) is dependant on the radius of the perfect ground plane.

In order to address the effects of the ground on a vertical monopole independent of any perfect (or imperfect) ground system, a perfectly conducting "base plate" radius of a = .001λ, representing a small conducting plate (with η = 0) at the base of the antenna, is assumed. This was chosen to match the same value used by Maley, et al, who generated a large body of data for ΔZ in reference [3], based on Wait's theory in [1]. At 18 MHz, the frequency chosen for the field testing of the theory, this works out to be approximately 1.651 cm. Since the most significant contributions from the ground to the antenna impedance occur closest to the antenna, as much of that area as possible was included in the calculations.

Figures 3.3a, 3.3b and 3.3c were generated using (3.1) to illustrate the relation between the change in input impedance with increased monopole height. ΔZ is again normalized with respect to ground impedance.

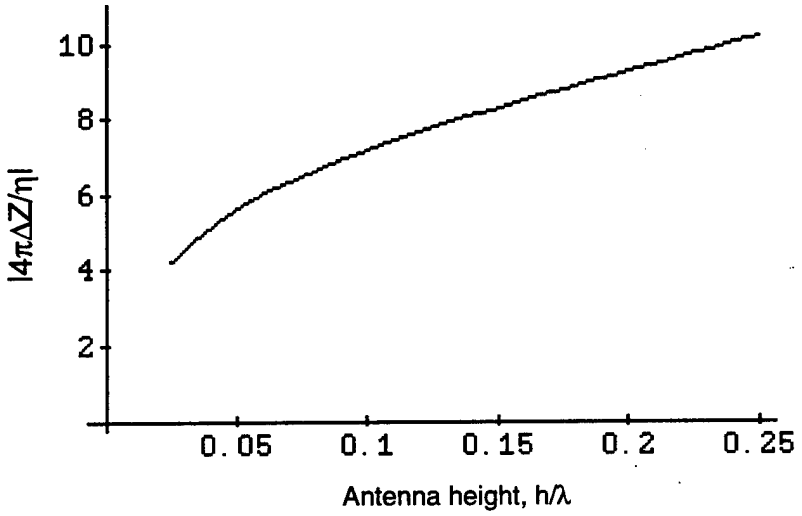


Figure 3.3a: The incremental input impedance of a vertical monopole over an imperfect ground normalized with respect to the ground impedance, η, as a function of the antenna height, normalized with respect to wavelength. Base plate radius a = .001λ.

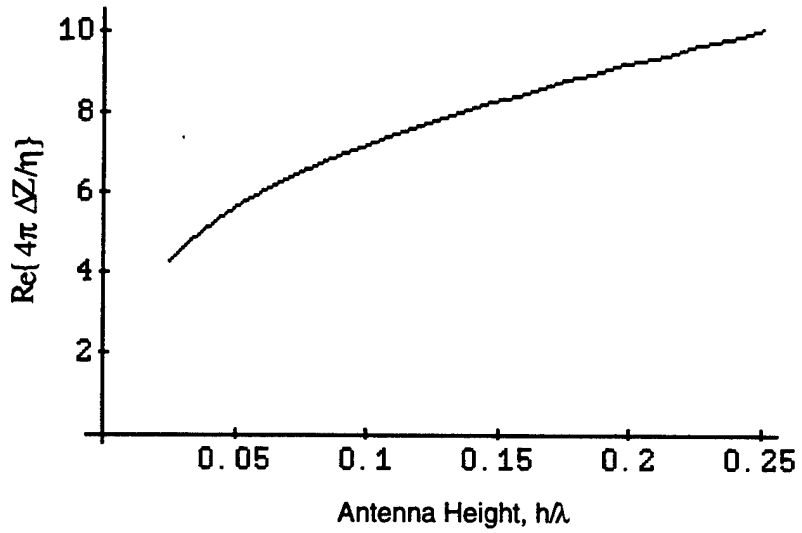


Figure 3.3b: The incremental input resistance of a vertical monopole over an imperfect ground, normalized with respect to the ground impedance, $\eta$, as a function of the antenna height, normalized with respect to wavelength. Base plate radius a = .001$\lambda$.

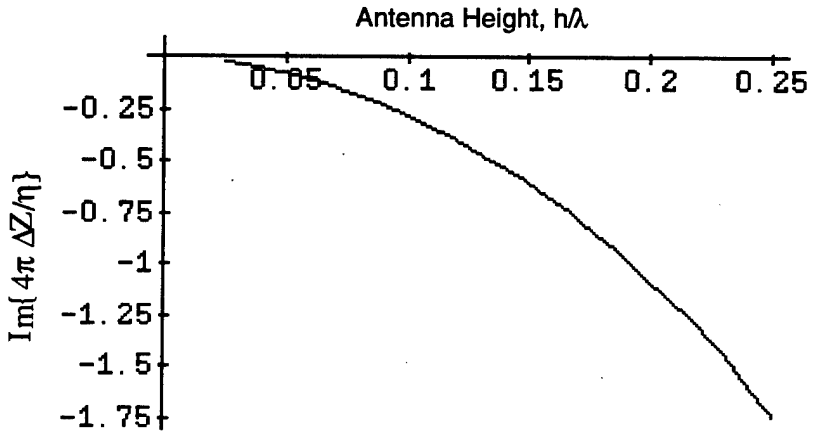


Figure 3.3c: The incremental input reactance of a vertical monopole over an imperfect ground, normalized with respect to the ground impedance, $\eta$, vs. the normalized antenna height. Base plate radius a = .001 $\lambda$.

Normally, monopole performance improves considerably as the height is increased. However, Fig.s 3.3b and 3.3c show that there is a corresponding increase in the ohmic resistance, $\Delta R$, and in the capacitive reactance, $-\Delta X$, with increased antenna height caused by losses in the ground, resulting in reduced

antenna efficiency.

To obtain a complete picture, one must incorporate the ground characteristics of the antenna site into the $\Delta Z$ calculations. As stated in Section II, the ground constants of conductivity and relative dielectric constant can be combined into a single function, $\delta$, as was done by Maley in [3]. The relation between the ground impedance and the constant $\delta$, referred to as the "ground factor ", is repeated below:

$$\eta = \sqrt{\frac{j\mu\omega}{\sigma + j\omega\varepsilon}} = \sqrt{j}\ \eta_o\,\delta \qquad (3.2)$$

where $\delta$ is defined as:

$$\delta = \frac{\delta'}{\sqrt{1 + j(\delta')^2\varepsilon_r}} = |\delta|\,e^{-j\psi} \qquad (3.3)$$

with:

$$\delta' = \sqrt{\frac{\omega\varepsilon_o}{\sigma}}$$

$$\psi = \frac{1}{2}\tan^{-1}[(\delta')^2\varepsilon_r]$$

with $\varepsilon_r$ being the relative dielectric constant for the ground plane. $\psi$ is referred to as the phase of the ground factor. Note that $|\partial| < 1/\sqrt{\varepsilon_r}$.

From measurements made in August of 1990 at a field site located at Waldorf, MD, $\delta$ was calculated to be approximately 0.25, and $\psi$ was calculated to equal 0.47 radians (27 degrees). The condition for the theoretical expressions in Section II, equation (2.5), was that the propagation constant in the ground must be much greater than that for free space:

$$\left|\sqrt{j\mu\omega\sigma - \omega^2\mu\varepsilon}\right| >> \omega\sqrt{\mu_o\varepsilon_o} \qquad (2.5)$$

$$11.92\sqrt[4]{\sigma^2 + .000169} >> 0.377$$

For $\sigma$ = .00941 (from the measurements at the Waldorf site), the left side of the

above condition is calculated to be 1.507, which is barely four (4) times 0.377. Therefore, the ground constants of the Waldorf site do not quite mean the condition for approximation. However, they were much closer than any of the other sites measured. Therefore, the ground constants from the Waldorf measurements are used through much of this section, unless noted otherwise, on the assumption that they were sufficient for illustration of the theory.

The figures that follow illustrate the relationship between $\Delta Z$ and variations in the ground represented by the ground factor terms $\delta$ and $\Psi$. Figures 3.4 and 3.5 show the change in impedance for an excellent ground ($\delta$=0.03, $\Psi$=0) and a poor ground ($\delta$=0.25, $\Psi$=0.471 radians). The $\delta$ and $\psi$ from Waldorf site represent the poor ground.

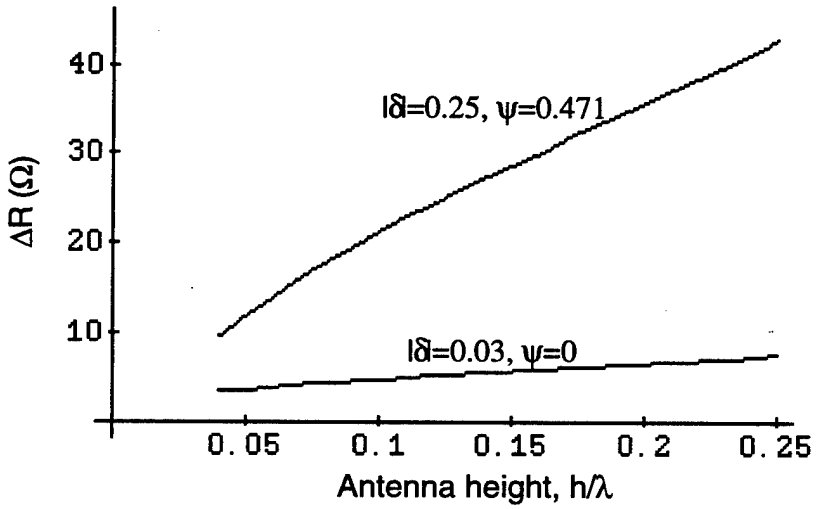


Figure 3.4: The input resistance increment of a vertical monopole over an imperfect ground as a function of the normalized antenna height, for an excellent ground ( $\delta$=0.03) and a ground type surveyed in the Waldorf, MD area. Base plate radius a = .001 $\lambda$.

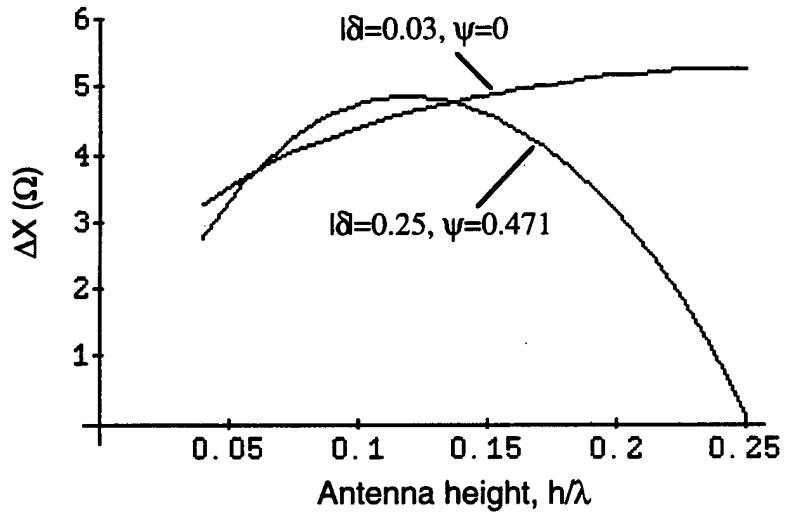


Figure 3.5: The input reactance increment of a vertical monopole over an imperfect ground as a function of the normalized antenna height, for an excellent ground ( $\delta$=0.03) and a ground type surveyed in the Waldorf, MD area. Base Plate radius a = .001$\lambda$.

Curves for the incremental impedance response as a function of the ground factor were also generated. Since $\delta$ and $\Psi$ are not independent, one must change $\Psi$ as $|\delta|$ is varied. To keep $\delta$ and $\Psi$ consistent, one method is to specify the two ground parameters ($\sigma$ and $\varepsilon_r$) and "sweep" the frequency through the HF band. A second method involves varying $|\delta|$ and computing the phase $\Psi$, using that $|\delta|$ along with a specified $\varepsilon_r$. This latter method is used to generate Figures 3.6 and 3.7. The $\varepsilon_r$ is taken from experimental results of ground samples at Waldorf in the HF band. (The results presented later in Appendix B show that the $\varepsilon_r$ changes little as the frequency increases above 5 MHz.) A plot of $\Psi$ generated as a function of $|\delta|$, with a specified $\varepsilon_r$ of 13, is shown in Figure 3.8.

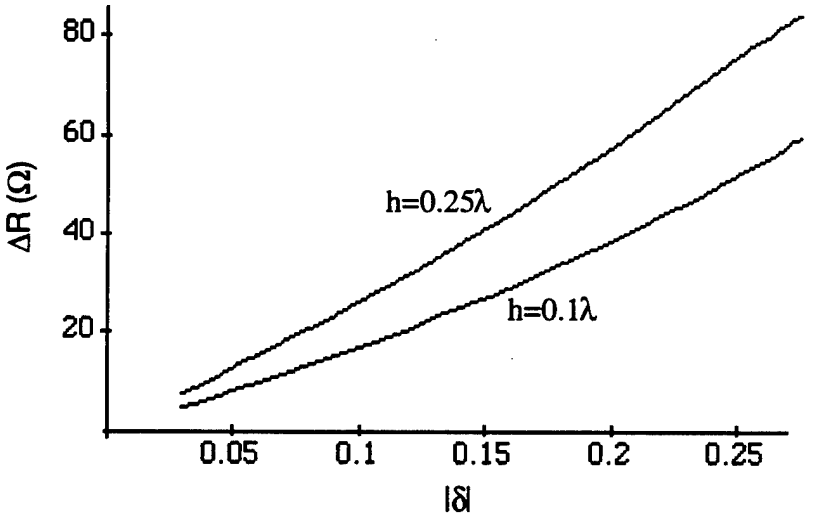


Figure 3.6: The input resistance increment for a vertical monopole over imperfect ground, as a function of the ground impedance factor, $|\delta|$, for $h=0.25\lambda$ and $h=0.1\lambda$. Note that the ground factor phase $\psi$ varies as a function of $|\delta|$, and a relative dielectric constant ($\varepsilon_r$) of 13 has been assumed throughout.

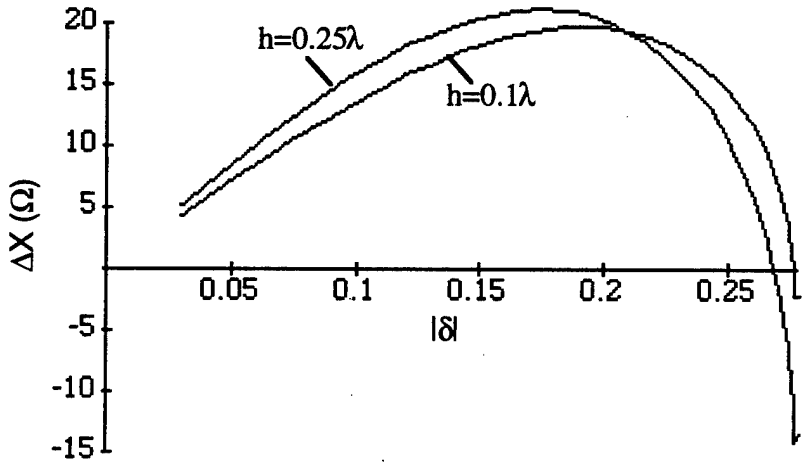


Figure 3.7: The input reactance increment for a vertical monopole over imperfect ground, as a function of the ground impedance factor, $|\delta|$, for $h=0.25\lambda$ and $h=0.1\lambda$. Note that the ground factor phase $\psi$ varies as a function of $|\delta|$, and a relative dielectric constant ($\varepsilon_r$) of 13 has been assumed throughout.

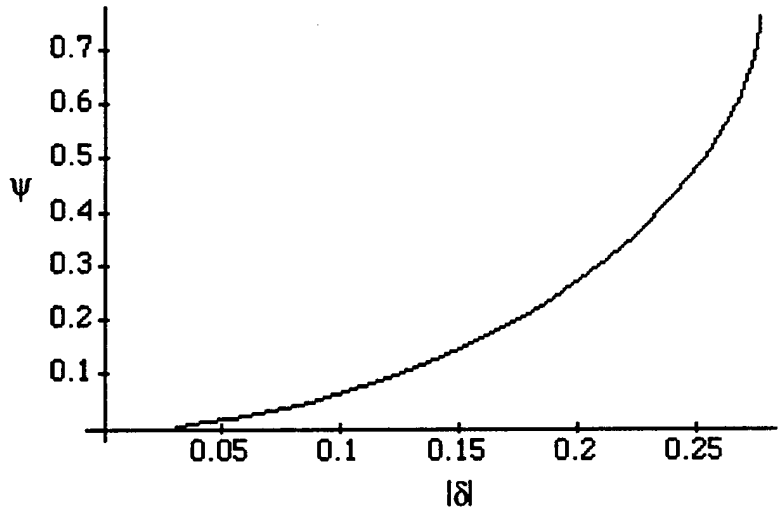


Figure 3.8: The ground impedance phase term $\psi$, as a function of the ground impedance factor magnitude, $|\delta|$. The relative dielectric constant $\varepsilon_r = 13.0$. (This $|\delta|$ and its corresponding $\psi$ were used to generate Figures 3.6 and 3.7.)

One observation is the low level of $\Delta X$ for a wide range of antenna heights and ground types, especially when one considers the high reactance inherent to a short ($0.1\lambda$) monopole. With respect to the $\Delta R$ curves, one observation is that as the antenna height increases, more power is radiated, causing more power to be absorbed by the ground, thereby increasing the resistive effects of the earth.

To further illustrate the ground effects on monopole impedance, the following three-dimensional plots are presented. Figures 3.9 and 3.10 show $\Delta R$ and $\Delta X$ for a quarter-wave monopole as a function of the ground factor magnitude and phase, $|\delta|$ and $\Psi$. Here, $|\delta|$ and $\Psi$ were treated in the analysis as independent variables, however, this is not actually the case. Therefore, there are portions of the curves at the limits of $|\delta|$ and $\Psi$ that are not physically realizable. One can see in Figure 3.9 that $|\delta|$ affects the change in resistance appreciably, while the phase $\Psi$ has very little effect. The opposite is true for Figure 3.10, where $\Psi$ appears to have great effect, especially for smaller values of $|\delta|$. This agrees with Maley's conclusions in [3].

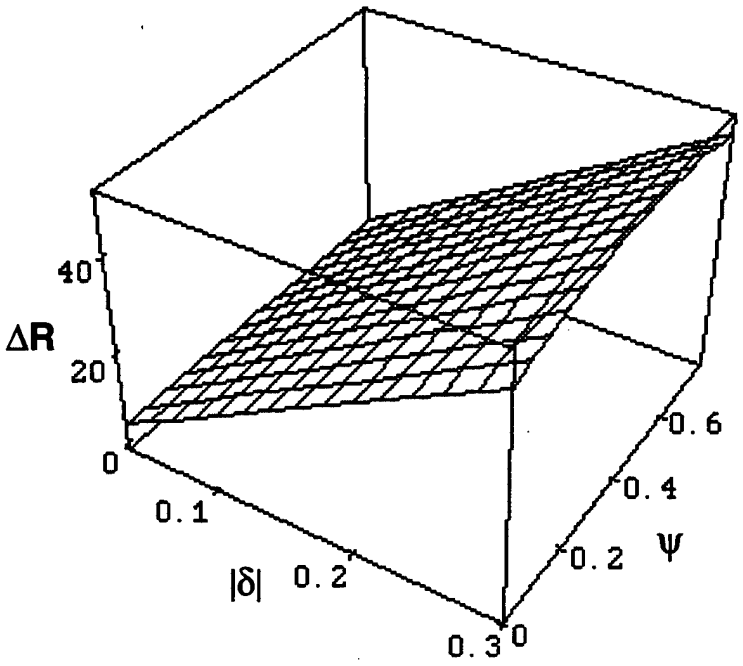


Figure 3.9: The incremental change in resistance for a quarter-wave monopole as a function of $|\delta|$ and $\psi$, the ground impedance factor magnitude and phase, treated as independent variables. (Note that sections of the graph may not correspond to realizable ground parameters.)

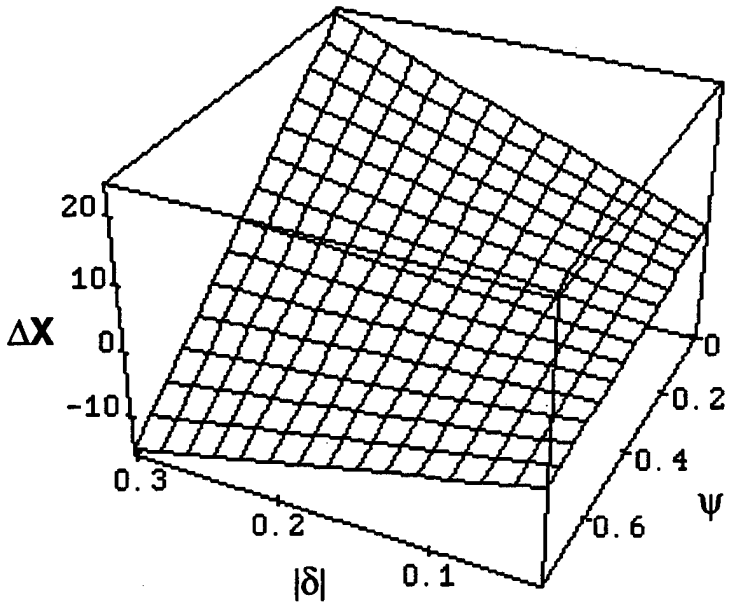


Figure 3.10: The incremental change in reactance for a quarter-wave monopole as a function of $|\delta|$ and $\psi$, the ground impedance factor magnitude and phase, where $|\delta|$ and $\psi$ are treated as independent variables. (Note that sections of the graph may not correspond to realizable ground parameters.) The plot was done with the $\psi$ axis reversed for graph clarity.

Another method of presenting the data is to show the change in impedance based on the ground parameters $\sigma$ and $\varepsilon_r$. Since the ground impedance is also a function of frequency, 18 MHz was chosen to generate Figures 3.11 and 3.12. Upon closer examination of equation (3.2), it can be shown that if the conductivity is increased (or decreased) by the same factor as the frequency, then $\delta'$ remains unchanged, and the resulting ground impedance term stays the same. Therefore, one could scale the plots shown in Figures 3.11 and 3.12 to the desired frequency by multiplying the conductivity axis by the same factor as for the frequency change.

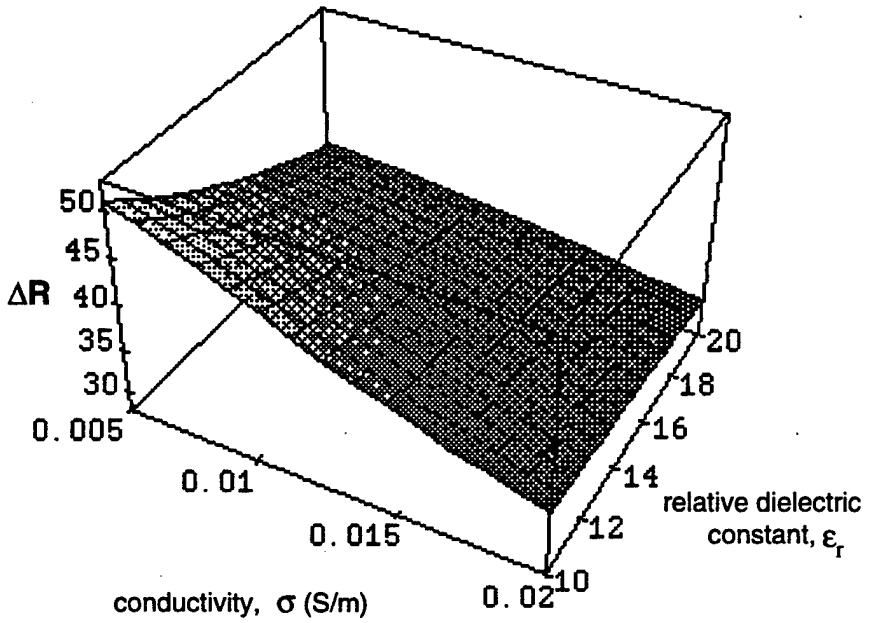


Figure 3.11: The incremental input resistance of a quarter-wave vertical monopole over an imperfect ground, as a function of the conductivity and relative dielectric constant of the surface. Frequency = 18 MHz.

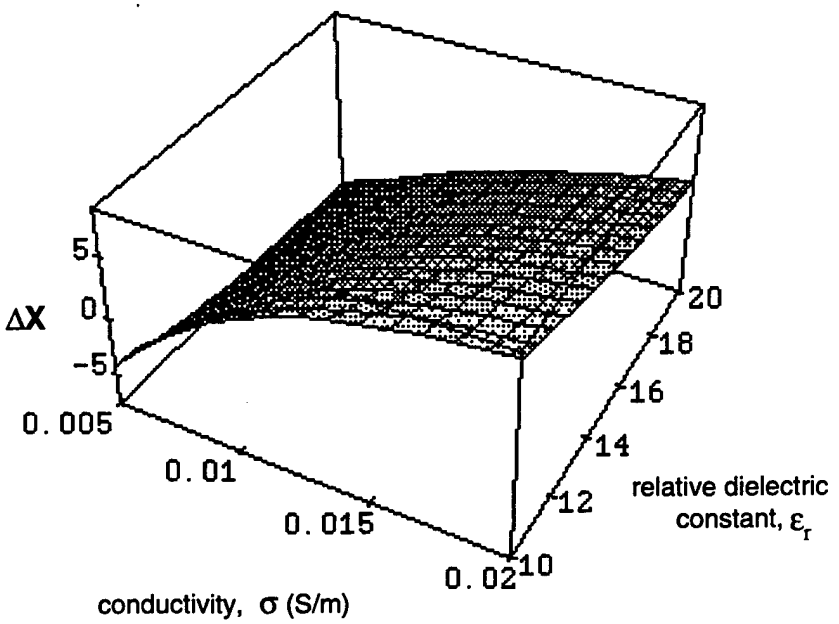


Figure 3.12: The incremental input reactance of a quarter-wave vertical monopole over an imperfect ground, as a function of the conductivity and relative dielectric constant of the surface. Frequency = 18 MHz.

## Computer Modeling of a Vertical Monopole

To this point, the report has focused on $\Delta Z$, the change in impedance from an imperfect (Z) to perfect ($Z_O$) ground. The next step is to predict what values of $Z_O$ one can expect for a particular monopole. This is accomplished by using the Numerical Electromagnetic Code, or NEC [6], a user-oriented computer code for the analysis of an antenna's electromagnetic behavior. A model of the antenna is constructed with special lines of code in the input file to the program representing wires, patches, antenna excitation, or the loading of the structure. The models may be assembled in free space or over a uniform ground.

One input requirement for the NEC computation is a particular operating frequency (or set of frequencies) for the antenna. A representative frequency of 18 MHz was selected from the HF band, with the structures scaled accordingly. The HF band was chosen because of the ease of modeling, and of existing test equipment for that band.

Table 3.1 shows the results of the NEC computation of the input impedance for a vertical monopole over a perfect ground. The input impedances of the same antennas over an imperfect ground were generated with NEC by using a special routine called the Sommerfeld-Norton method, which allows one to enter specific values for the conductivity and dielectric constant of the ground plane below the antenna. Ground constant values from measurements made at NRL's Waldorf site were used to obtain the results shown in Table 3.2.

| Antenna # | Height (m) | R (ohms) | X (ohms) |
|---|---|---|---|
| 1 (0.1λ) | 1.667 | 4.79 | -376.3 |
| 2 (0.15λ) | 2.5 | 10.93 | -202.8 |
| 3 (0.2λ) | 3.333 | 21.38 | -86.1 |
| 4 (0.25λ) | 4.167 | 38.74 | 13.2 |

Table 3.1: The input impedance of a vertical monopole over a perfect ground at 18 MHz, as predicted by the Numerical Electromagnetics Code (NEC).

| Antenna # | Height (m) | R (ohms) | X (ohms) |
|---|---|---|---|
| 1 (0.1λ) | 1.667 | 124.67 | -544.5 |
| 2 (0.15λ) | 2.5 | 125.9 | -360.1 |
| 3 (0.2λ) | 3.333 | 141.3 | -249.1 |
| 4 (0.25λ) | 4.167 | 162.77 | -156.87 |

Table 3.2: The input impedance of a vertical monopole over an imperfect ground at 18 MHz, as predicted by the Numerical Electromagnetics Code (NEC). Ground conductivity is 8.99 mmho/m, and $\varepsilon_r$ is 12.51.

Examining the differences between the results of the two tables ($\Delta R$ and $\Delta X$), it can be seen that there is a significant difference between the values predicted for $\Delta Z$ by theory and those generated by NEC. A contributor to the disparity between the predicted and NEC-generated values of $\Delta X$ is that the ground constants used do not quite meet Wait's criteria (that the propagation constant in the ground must be much greater than that for free space) for the approximations used in the theory developed in Section II. In addition, the model was based on the antenna used in the experimentation, which may not have been the best approximation of an infinitesimally thin monopole, for which the theory was derived.

Impedance values that were derived from the NEC model for the antenna over perfect ground provided data that was very similar to the measured data. However, the model over imperfect ground produced impedance values much different from the experimental results. Because of the disparity between the calculated theoretical and experimental results and those produced by the NEC model for the imperfect ground, the NEC modeling over an imperfect ground was not pursued further. For comparisons between perfect and imperfect ground, as well as between imperfect ground and the effects of a ground screen (Section V), experimental results for the impedance of an imperfect earth are used.

## IV. Experimental Investigation of the Ground Effects on a Vertical Monopole

Field measurements were performed to verify the computer-generated results of the theories set forth by Wait [1]. Input impedance tests were conducted on vertical monopoles at frequencies in the HF band during October 1990. The HF band was chosen so that antenna and ground screen sizes would be small enough to be easily handled, but not so small that slight imperfections in antenna construction would affect the results. In addition, both conductivity and relative permitivity of the sites measured stabilized between 5 and 30 MHz. Antenna measurements were conducted over three surfaces: perfect ground, imperfect ground, and imperfect ground with a radial ground screen. The work performed with the perfect and imperfect grounds (no ground screen) is documented in this section. Measurements taken over a radial ground screen are descibed in Section V.

### A. Method

Measurements were conducted with four vertical monopoles of different heights. To simplify the experimentation, none of the antennas were fitted with top loading, i.e., wires extended from the top of the monopole (horizontally, or as part of the guying assembly). Top loading is added to monopoles to increase the effective height of the structure. In addition, measurements were done at a single frequency, 18 MHz. This was done so that the ground constants (dependant on frequency) would be consistant for each antenna height , as well as for simplicity.

In preparation for doing antenna impedance measurements over an imperfect ground, site surveys were conducted at three locations. The parameters measured were the ground conductivity and the relative dielectric constant. These were measured at a number of locations at each site to gauge the variability of the ground constants within the intended test area, and to see if those parameters met the criteria set forth by Wait in [1]. These efforts were documented in Appendix B. From these surveys, an NRL site located in Waldorf, MD was selected for conducting tests.

The impedance measurements were perfomed using a Hewlett Packard (HP) model 4195 Network Analyzer. To measure the impedance of the monopole, it was

necessary to place the test equipment at some distance from the antenna, so that the presence of the network analyzer would not affect the performance of the ground screen or couple with the antenna mast. The HP4195 has the capability to calibrate out the effects of the coaxial cable, enabling it to measure the input impedance at the base of the antenna automatically.

To make an antenna that corresponded as closely to the theoretical description as possible (therby easier to model), the base for the test monopoles was constructed of wood. The base was made up of a plywood square with four arms (2 by 4's) which were bolted together. A wooden dowel was mounted in the center, over which the test monopoles were placed. The base connection was accomplished with a hose clamp (which simplified the changing of antennas), from which a wire was run to the center pin of a type-N coaxial connector. A ground strap with an alligator clamp was attached to the shield of the connector for connecting the coaxial shield to the ground plane.

## B. Field Measurements

### Monopole over "Perfect" Ground Screen

Since the focus of this report concerns the change in antenna impedance between a perfect and an imperfect ground plane, measurements of monopole input impedance were made above a "perfect" ground system at NRL's Brandywine field site. This site consists of a large steel table mounted on a pedestal, which can be lowered to the laboratory space underground. When the table is raised to be flush with the surface, it connects to a large ground screen approximately 122 m (400 ft.) in diameter. Seventy-two radials extend outward from the ground screen to a total diameter of 304.8 m (1000 ft.). Excellent correlation between measurements made at Brandywine and computer models of antennas over perfect ground has been observed at frequencies above 7 MHz [9]. A diagram of the test configuration is shown in Figure 5.1.

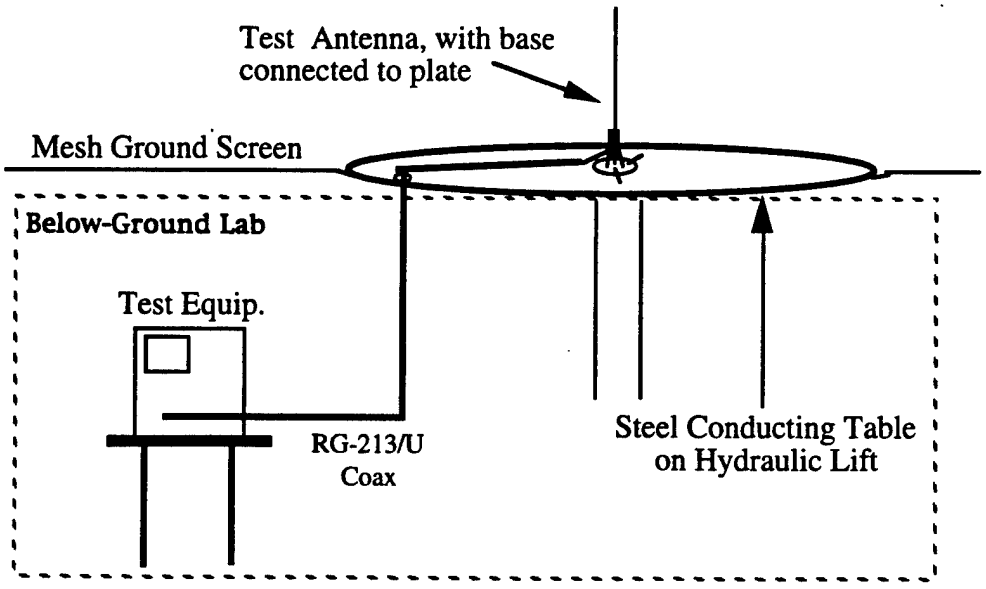


Figure 4.1: Test configuration at NRL Brandywine Field Site. Ground Screen comprises 1/2-inch mesh hardware cloth out to a 61 m radius, with 72 radials extending to a 152.4 m radius from the table.

Four monopole heights were measured for input impedance at a frequency of 18 MHz, and the results are shown in Table 5.1. Measurements were taken using an HP4195 Network Analyzer in the Network configuration. A full calibration was performed on the 35 ft. coaxial cable before each set of measurements. Antenna #1 was a single section of 5/8" aluminum tubing. A single telescoping aluminum whip was used to represent antennas #2-#4. This whip has a maximum height of 5.5 m (18 ft.) and a minimum height of 1.86 m (6.1 ft.). The various sections of the whip were marked for each height to add consistency between the different sets of measurements. The readings shown below were visually "averaged" from a number of swept measurements for each antenna.

| Ant. # | Height (m.) | $Z_{in}$ - Set 1 R(Ω) | $Z_{in}$ - Set 1 X(Ω) | $Z_{in}$ - Set 2 R(Ω) | $Z_{in}$ - Set 2 X(Ω) | $Z_{in}$ - Set 3 R(Ω) | $Z_{in}$ - Set 3 X(Ω) |
|---|---|---|---|---|---|---|---|
| 1 (0.1λ) | 1.666 | 11.3 | -318.0 | 10.5 | -314.2 | 10.6 | -313.6 |
| 2 (0.15λ) | 2.5 | 17.2 | -183.2 | 16.5 | -181.5 | 16.5 | -179.4 |
| 3 (0.2λ) | 3.333 | 23.15 | -118.8 | 22.3 | -117.8 | 22.4 | -117.1 |
| 4 (0.25λ) | 4.167 | 48.7 | 10.9 | 48.4 | 12.15 | 48.1 | 12.55 |

Table 4.1: Three sets of measurements of the input impedance of a vertical monopole at 18 MHz over a perfect ground system at Brandywine, MD. The measurement Resolution Bandwidth = 3 kHz.

## Monopole Over Imperfect Ground

Measurements were conducted at NRL Waldorf Lower Field Site, on an open field whose useable area was approximately 53 m square. Although the field was much larger, the useable area was limited by trees, metal fencing and piping beneath the ground. A diagram of the test site is shown in Figure 2.

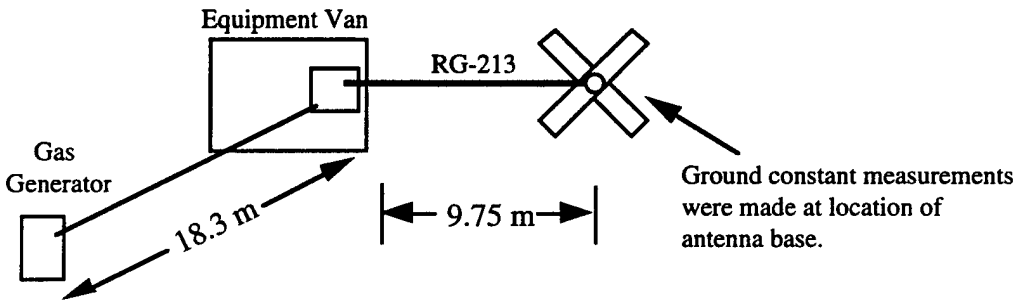


Figure 4.2: Test configuration at NRL Waldorf Lower Field Site. Antenna base at center placed on bare dirt. A ground strap connects the shield of the type-N connector to ground. Metal fence is approximately 30 m distant from center of circle.

A measurement of the ground constants at the location selected for the antenna base was conducted before the antenna was set up. The results of that survey are given below in Table 4.2. The conductivity σ and relative dielectric constant $\varepsilon_r$ were calculated using the method detailed in Section IV.

| Freq.(MHz) | $X_o$ (Ω) | R (Ω) | X (Ω) | $\varepsilon_r$ | σ (mS) |
|---|---|---|---|---|---|
| 17.00 | -1250 | 49.35 | -56.85 | 12.54 | 10.28 |
| 17.50 | -1200 | 48.15 | -55.4 | 12.34 | 10.43 |
| 18.00 | -1135 | 46.85 | -53.85 | 12.0 | 10.44 |
| 18.50 | -1095 | 45.65 | -52.35 | 11.88 | 10.65 |
| 19.00 | -1060 | 44.55 | -50.7 | 11.80 | 10.94 |

Table 4.2: Results of a ground impedance survey at Waldorf Lower Field site on 10/12/90. Measurements of $X_o$, R and X were done with an HP 4195 Network Analyzer and a Monopole Probe. The relative dielectric constant and conductivity were calculated using the method outlined in Section IV.

Recalling the constraint put forth by Wait for the ground impedance that $|\gamma| >> \beta$, given as equation (2.5) in Section II:

$$\left|\sqrt{i\mu\omega\sigma - \omega^2\mu\varepsilon}\right| >> \omega^2\sqrt{\mu_o\varepsilon_o} \qquad (2.5)$$

where the quantity on the left side is the propagation constant through the ground, and the right side is the propagation constant through free space. Substituting the values for σ and $\varepsilon_r$ from Table 4.2 into equation (2.5), the ratio $|\gamma|/\beta$ was found to be equal to 4.1, rather than 10 or greater, so the theoretical constraint was not met. Since this area was the closest to meeting the condition of the three sites surveyed in the local area, it was selected for the experimental measurements.

Once the ground measurements were completed, the antenna base was put in place, and two sets of antenna measurements were conducted. The antennas measured here were identical to those in Table 4.1, which were used at the Brandywine site. The results are given in Table 4.3.

| Antenna # | Height (m) | $Z_{in}$ - Set 1 R(Ω) | X(Ω) | $Z_{in}$ - Set 2 R(Ω) | X(Ω) |
|---|---|---|---|---|---|
| 1 (0.1λ) | 1.667 | 74.0 | -368.5 | 66.4 | -362.0 |
| 2 (0.15λ) | 2.5 | 81.5 | -212.3 | 76.5 | -210.8 |
| 3 (0.2λ) | 3.33 | 95.2 | -105.1 | 84.2 | -142.4 |
| 4 (0.25λ) | 4.167 | 115.3 | -10.8 | 112.1 | -10.9 |

Table 4.3: Two sets of measurements of the input impedance of a vertical monopole at 18 MHz over an imperfect ground system at Waldorf, MD. Measurements were taken using an HP4195 Network Analyzer in the Network configuration with a Resolution Bandwidth of 3 kHz.

The goal is to compare measurements of monopoles with values calculated using the theory set forth in Section II. Table 4.4 shows the change in impedance as calculated for a vertical monopole from an imperfect to a perfect ground, along with the experimental results for ΔZ. The experimental values for ΔZ were taken from the difference between Set 2 at the Waldorf site and Set 1 at the Brandywine site because this combination gave the results that were closest to theory. Recall that $\Delta Z = Z_{\text{imperfect gnd.}} - Z_{\text{perfect gnd.}}$

| Antenna # | Predicted ΔZ ΔR | ΔX | Measured ΔZ ΔR | ΔX |
|---|---|---|---|---|
| 1 (0.1λ) | 58.56 | 19.68 | 55.1 | -44.0 |
| 2 (0.15λ) | 67.1 | 20.24 | 59.3 | -27.6 |
| 3 (0.2λ) | 74.76 | 19.31 | 61.05 | -23.6 |
| 4 (0.25λ) | 82.48 | 16.81 | 63.4 | -21.8 |

Table 4.4: The change in impedance of a vertical monopole from over an imperfect to a perfect ground, from theoretical predictions using the theory from Section II and antenna measurements. Base plate radius a for predicted ΔZ = .0006λ.

A comparison of the predicted and measured ΔZ shows that the values for ΔR are relatively close, while the values for ΔX are quite different. Recalling Figure 3.5, its predicted ΔX curve for the case of the poor ground is much different than the curve for the good ground. Table 4.4 shows that when the ground conductivity goes below the level defined in Wait's constraint (equation 2.5), the contribution of the ground to the input reactance of the antenna departs from the theory presented here. From Table 4.4, it appears that the ground at Waldorf contributes to the capacitive reactance of the vertical monopole, rather than decreasing it as predicted in theory (i.e., effectively contributing a negative rather than a positive reactance to the input impedance).

Given the values for the measured values for $\Delta R$ in Table 4.4, calculations were performed to determine the lower limit of integration for the expression for $\Delta Z$ (equivalent to the antenna base plate radius) that would produce an equivalent computed $\Delta R$ for a particular antenna height. The base plate radius "a" used in generating Table 4.4 is $0.0006\lambda$, equal to 1 cm at 18 MHz. This approximates the radius of the aluminum monopole. The estimated "effective" base plate radii for the four antenna heights examined are given in Table 4.5.

| | Measured | Adjusted calc. | | Effective Base Radius | |
|---|---|---|---|---|---|
| Antenna # | $\Delta R$ | $\Delta R$ | $\Delta X$ | $(a/\lambda)$ | (cm) |
| 1 ($0.1\lambda$) | 55.1 | 55.08 | 18.38 | 0.00077 | 1.283 |
| 2 ($0.15\lambda$) | 59.3 | 59.27 | 17.31 | 0.00105 | 1.75 |
| 3 ($0.2\lambda$) | 61.05 | 61.00 | 14.16 | 0.0016 | 2.667 |
| 4 ($0.25\lambda$) | 63.4 | 63.5 | 9.68 | 0.0024 | 4.0 |

Table 4.5: The Effective antenna base plate radius ($a/\lambda$) for a vertical monopole which produces a computed $\Delta R$ identical to the $\Delta R$ measured in the field. The base used in the measurements was non-conducting, and the radius of the monopole was approximately 1 cm.

One suggestion for the difference between the effective base radii and the radius of the monopoles measured is that as the antenna electrical length approaches a quarter-wave monopole, its impedance approaches a purely real value. As a result, the contributions from the input connector, hose clamp and ground strap may become slightly more significant.

A number of factors contributed to the overall discrepancy between the theoretical and experimental $\Delta Z$'s presented in Table 4.4. Some of these are inaccuracy in the calibration of the network analyzer, transient behavior in the coaxial cable, possible capacitive contributions when using the telescoping whip, the effects of a non-homogeneous ground, and human error. It should also be noted that, due to equipment problems, the network analyzer was measuring the antenna impedances in the Network configuration rather than the more accurate Impedance configuration.

## V: Experimental Investigation of the Effects of a Ground Screen over an Imperfect Ground on a Vertical Monopole

Experiments were conducted to verify the calculated results (based on Wait's theory in [3]) for the change in impedance ($\Delta Z$) of a vertical monopole from over an imperfect ground screen to over a perfect ground. Input impedance measurements on vertical monopoles over radial ground screens and over a "perfect" ground plane were conducted during August of 1990. The following is documentation of those efforts, which are then compared with the calculated results.

### I. Method

The experiments were conducted to provide a set of data points comparable to calculated results, so that a direct comparison could be made. The variables in the experiments were the antenna height and the radius of the ground screen. To simplify the measurements, no top loading was introduced, and the thickness of the ground screen wires was held constant. The frequency of choice (as previously stated) was the mid-HF band. There is a difficulty in doing any sort of field impedance measurements because of the rather crowded and noisy electromagnetic environment at HF (up through VHF). External electomagnetic sources at the test frequency incident on the antenna can seriously affect the measurement of that antenna's impedance.

In constructing a test antenna, a permanent base insulator was attached to a circular aluminum plate approximately 1/2 m in radius. The monopoles were hollow aluminum rods cut to proper lengths; these were then mounted to the base insulator. This allowed the changing of antenna heights while leaving the ground screen under test undisturbed. A number of antenna heights were used, along with different frequencies, so that a number of data points could be taken without having to change the physical length of the ground radials frequently. The monopole heights used were $.1\lambda$ and $.05\lambda$, and were represented using four different antennas at two different frequencies. By changing the length of the ground radials once, four data points for each representative ground screen could be obtained. An outline of the testing conducted is given in Table 5.1.

| Ant. # | Antenna height (λ) | (m) | Screen radius (λ) | (m) | Frequency (MHz) |
|---|---|---|---|---|---|
| 1 | 0.1 | 2.5 | 0.2 | 5.0 | 12.0 |
| | | | 0.0667 | 1.667 | 12.0 |
| 2 | 0.1 | 1.667 | 0.3 | 5.0 | 18.0 |
| | | | 0.1 | 1.667 | 18.0 |
| 3 | 0.05 | 1.25 | 0.2 | 5.0 | 12.0 |
| | | | 0.0667 | 1.667 | 12.0 |
| 4 | 0.05 | 0.833 | 0.3 | 5.0 | 18.0 |
| | | | 0.1 | 1.667 | 18.0 |

Table 5.1: A listing of the antennas used in the monopole impedance tests, with their physical and electrical heights and the general frequency at which they were measured.

The Waldorf site was bounded at one end by a metal fence, and the test monopole was set up at least one wavelength distant.

The test equipment used to measure the impedance of the monopole was placed 18.3 m from the antenna, so that its presence would not affect the performance of the ground screen or couple with the antenna mast. Two methods of impedance measurement were used: one required an HP4195 Network Analyzer, and the other method used a General Radio RF Bridge (GR bridge) along with a signal source and a detector. The HP4195 has a capability to calibrate out the presence of the coaxial cable, enabling it to produce the input impedance at the base of the antenna automatically. The GR bridge had no such capability, and theoretical methods were required to transform out the effects of the cable on the measured impedance. It was hoped that the GR bridge would provide the accuracy and resolution needed for the resistive part of the impedance, and that the HP4195 would give similar accuracy for the much larger reactive part of the impedance.

Two different methods were attempted for "deimbedding" the impedance measurements made with the GR bridge. These methods used distributed parameters to transform out the effects of the coax on the measurement.

Method 1:

The distributed parameters (resistance, conductance, inductance and capacitance per unit length) of a coaxial cable are calculated from the following:

$$r = \sqrt{\frac{f\mu_o}{4\pi\sigma}}\left(\frac{1}{a}+\frac{1}{b}\right) \qquad g = \frac{2\pi\omega\varepsilon_o\varepsilon_r\tan\delta}{\ln(b/a)}$$

$$L = \frac{\mu_o}{2\pi}\ln(b/a) \qquad c = \frac{2\pi\omega\varepsilon_o\varepsilon_r}{\ln(b/a)}$$

where a and b are the inner and outer conductor radii. The units are mks, and the unit length is one meter.

From the these distributed parameters, one may calculate the complex propagation constant $\gamma$ and the characteristic impedance, $Z_o$:

$$\gamma = \sqrt{(r+j\omega L)(g+j\omega c)}$$

$$Z_o = \sqrt{\frac{r+j\omega L}{g+j\omega c}}$$

These values are then inserted into the following expression for the antenna input impedance, which uses the ABCD (also called cascade or transmission) parameters for a lossy transmission line of length l:

$$Z_L = \frac{Z_{in}\cosh(\gamma l) - Z_o\sinh(\gamma l)}{(Z_{in}/Z_o)\sinh(\gamma l) - \cosh(\gamma l)}$$

Method 2:

The distributed conductance and resistance of the coaxial cable are found by using the Loss(dB)/100 ft. data supplied by the cable manufacturer at two frequencies close to the frequencies of measurement. Beginning with the expression

for the variation of the propagating wave:

$$V \cong \exp\left[ -\frac{1}{2} \left( \frac{R}{Z_o} \sqrt{f} + g Z_o f \right) l \right]$$

where:

l = length of line
f = frequency
r = resistance/unit length
g = conductance/unit length

Taking the log, we develop an expression for the power variation in dB:

$$P\,(dB) = 20 \log_{10}\left( \exp\left[ -\frac{1}{2} \left( \frac{R}{Z_o} \sqrt{f} + g Z_o f \right) l \right] \right)$$

$$P\,(dB) = 20 \log(e) \ln\left( \exp\left[ -\frac{1}{2} \left( \frac{R}{Z_o} \sqrt{f} + g Z_o f \right) l \right] \right)$$

$$P\,(dB) = -10 \log(e) \left( \frac{R}{Z_o} \sqrt{f} + g Z_o f \right) l$$

$$\text{Loss}\,(dB) = +10 \log(e) \left( \frac{R}{Z_o} \sqrt{f} + g Z_o f \right) l$$

$$\text{Loss}\,(dB)/l = K \left( \frac{R}{Z_o} \sqrt{f} + g Z_o f \right)$$

where K equals 4.343. Entering a value for the loss per unit length at two different frequencies produces two equations with two unknowns (r and g), which can be solved simultaneously.

To obtain the inductance/unit length, one uses the formula from Method 1. The capacitance/unit length is also given in the cable manufacturer specifications. In the case of RG-213 cable, (the cable used for these measurements) the calculated value for c from Method 1 was close to the number specified by the cable manufacturer, Belden Wire & Cable.

## II. Field Measurements

### Monopole over "Perfect" Ground Screen

Antenna measurements for the case of a perfect ground were made at the Brandywine Field Site, where there was a large steel table mounted on a pedestal (with laboratory space below) connected to a large ground screen approximately 122 m (400 ft.) in diameter. While at Brandywine, it was discovered that NRL's Network Analyzer (the HP4195) could only make measurements using the Network configuration, which gave impedances in addition to reflection coefficient data. These values are shown below with impedance measurements obtained by using another HP4195 operating in the Impedance configuration, which is a much more appropriate mode for this type of measurement. This second analyzer belonged to a contractor operating at Brandywine at the same time, but was only available for a short period. Therefore, data were only taken with two antennas using the network configuration. Those results are given below.

| Frequency | Input Impedance (R + jX)(Ω) | | | |
|---|---|---|---|---|
| (MHz) | Ant.1(2.5 m) | Ant. 2 (1.67 m) | Ant. 3 (1.25 m) | Ant. 4 (0.833 m) |
| 9.0 | 2.91 - j394.25 | 2.50 - j506.45 | 2.75 - j593.5 | 3.1 - j719.40 |
| 12.0 | 4.15 - j278.80 | 3.31 - j372.20 | 3.7 - j438.91 | 4.8 - j537.65 |
| 15.0 | 5.30 - j201.58 | 3.33 - j285.70 | 2.7 - j340.60 | 3.1 - j419.82 |
| 18.0 | 7.47 - j146.27 | 3.99 - j225.05 | 3.1 - j274.65 | 3.4 - j340.80 |

Table 5.2: Input Impedance of a vertical monopole over a perfect ground screen. Measured at NRL Brandywine Field Site, using a HP4195A Network Analyzer in the Impedance configuration. Values are visual average of ten or more measurement sweeps. Resolution Bandwidth=3 kHz

| Frequency (MHz) | Input Impedance (R + jX) (Ω) Ant.1 | Ant. 2 | Ant. 3 | Ant. 4 |
|---|---|---|---|---|
| 9.0 | - | 5 - j498 (+/-2) | - | 8 - j703 (4) |
| 12.0 | - | 3.3 - j365.5 (+/- 1.2) | - | 4 - j522 (4) |
| 15.0 | - | 4.5 - j284.4 (+/- 1) | - | 6 - j415.5 (3) |
| 18.0 | - | 4.2 - j225 (+/-.4) | - | 3.5 -j340.3 (2) |

Table 5.3: Input Impedance of a vertical monopole over a perfect ground screen. Measured at NRL Brandywine Field Site, using a HP4195A Network Analyzer in the Network configuration. Values are visual average of ten or more measurement sweeps. Numbers in parenthesis are the maximum normal variation of the measurements. Resolution Bandwidth=3 kHz

The values from both analyzers are quite close when considering Z as a whole. However, there are some big differences in R, especially at the lower frequencies. Differences of more than one ohm in the impedance could introduce an appreciable error when calculating $\Delta Z$. This can be attributed to X being very large compared to R, so that a very small variation (<2%) in a magnitude and/or phase measurement can seriously affect the resistive component of the impedance. Because of the conditions and the nature of the impedances of vertical monopoles, the NRL analyzer was deemed acceptable.

In Table 5.4, the results of the antenna measurements using the GR bridge configuration are given, using Methods 1 and 2 for deimbedding the input impedance. These are listed alongside the NEC predictions of impedance for the equivalent antenna at the same frequency. Note that the original NEC impedance predictions were calculated to be in parallel with the capacitance of the monopole base (approximately 16 pF), producing reactances quite similar to the values listed in Tables 5.2 and 5.3 taken from the HP4195.

| Antenna # (m) | Frequency (MHz) | Method 1 ($Z_L$, W) | Method 2 ($Z_L$, W) | NEC Model ($Z_L$, W) |
|---|---|---|---|---|
| 1 (2.5) | 12.01 | 53.66 + j825.76 | 123.99 - j506.82 | 2.11 - j266.74 |
| 2 (1.667) | 18.02 | 509.64 - j3022.9 | 34.8 - j229.48 | 1.81 - j222.41 |
| 3 (1.25) | 12.01 | 61.51 + j839.5 | 123.44 - j500.9 | 0.33 - j418.22 |
| 4 (0.833) | 18.00 | 545.1 - j2894.5 | 35.2 - j229.17 | 0.26 - j330.07 |

Table 5.4: Input Impedance of a vertical monopole over a perfect ground screen. Measured at NRL Brandywine Field Site, using a General Radio RF Bridge. Results were obtained by transforming out the effects of the 35 ft. length of coaxial cable between the Bridge and the antenna. Method 1 used the cable's dimensions to calculate the distributed parameters, while Method 2 used values from the attenuation and capacitance data provided by Belden Wire.

Comparing with Tables 5.2 and 5.3, Method 2 appears to be more successful than Method 1. Additionally, the NEC model tracks quite well with the network analyzer measurements. It is believed that the same difficulty in resolving such a small resistive component from the network analyzer was also a factor in the NEC analysis.

## Monopole On Radial Ground Screen Over Imperfect Ground

Measurements were conducted at NRL Waldorf Lower Field Site, the same site used for the measurements over imperfect ground with no ground screen. A diagram of the test site with the ground screen added is shown in Figure 5.2.

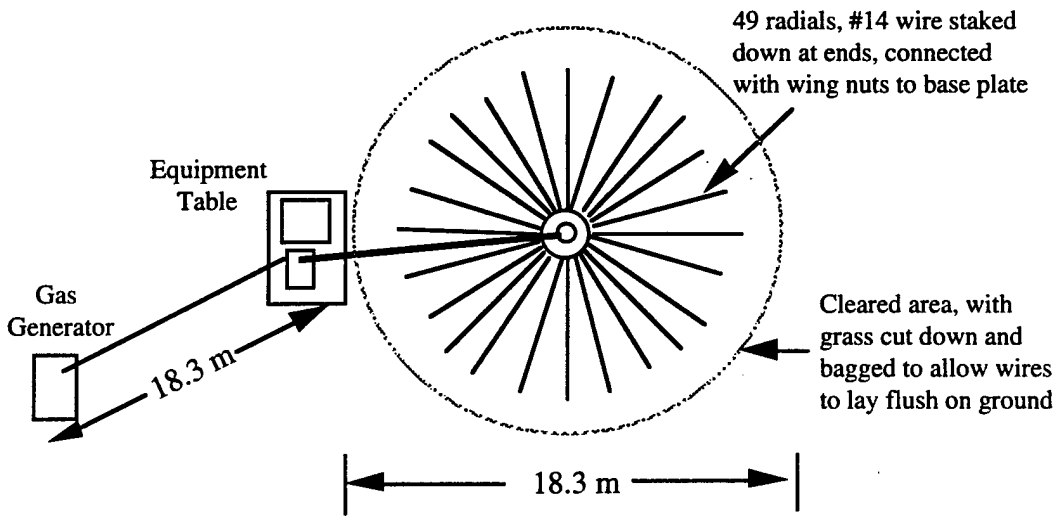


Figure 5.2: Test configuration at NRL Waldorf Lower Field Site. Antenna base at center placed on bare dirt. Metal fence approximately 30.5 m distant from center of circle.

Two different lengths of RG-213 cable were used, since some antennas proved impossible to measure when using the GR bridge. A metal shielded coaxial low-loss cable was also tried, but the impedance measurements were too sensitive to the cable's position and to any physical contact made with it.

Site preparation took approximately a day and a half. The site is an unused open field of grass which is cut once a month, so clearing a 18.3 m circle was required in order to get the ground wires as close to the surface as possible. A patch in the center was cleared down to bare dirt, and ground constant measurements were made from 8 to 20 MHz. These measurements were repeated the next morning, then the base was laid down and the ground radials were staked out. The initial radius of the ground screen (measured from the center of the plate, not the edge) was 5 m (see Table 5.1). The wires were also pressed to the surface of the ground around the base plate by using unfolded paper clips.

Over the next two days, measurements of the input impedance of the various monopoles (as listed in Table 5.1) were taken, using both the network analyzer and the GR Bridge. Problems occured while using the GR bridge. One problem was that the length of coax would transform the impedances at 18 MHz to values that exceeded the measurement capability of the GR Bridge. This required switching cables and re-calibrating the bridge. A second difficulty was the necessity of repeating each measurement a number of times. As the day progressed, the noise and interference from signals on or near the same channel would increase, making the nulls less sharp. Eventually, the data collected using the bridge were deemed unacceptable, and only the results taken from the network analyzer were documented.

Measurements with the network analyzer of the input impedance of the monopoles in Table 5.1 over two different sizes of ground screens are given below in Table 5.5. Table 5.6 gives the resultant $\Delta Z$'s from the network analyzer measurements over both perfect and imperfect ground, and these can be compared to Table 5.7, which shows predicted $\Delta Z$ for the same configurations using the theory in Section II.

| Ant. # | Ant. height (λ) | Ant. height (m) | Screen radius (λ) | Screen radius (m) | Frequency (MHz) | Input Impedance R(Ω) | Input Impedance X(Ω) |
|---|---|---|---|---|---|---|---|
| 2 | 0.1 | 1.667 | 0.3 | 5 | 18.0 | 4.05 (.25) | -215.65 |
| 1 | 0.1 | 2.5 | 0.2 | 5 | 12.0 | 3.4 (.4) | -275.5 |
| 2 | 0.1 | 1.667 | 0.1 | 1.667 | 18.0 | 5.25 (.35) | -255.85 |
| 1 | 0.1 | 2.5 | 0.0667 | 1.667 | 12.1 | 6.25 (.5) | -275.8 |
| 4 | 0.05 | 0.833 | 0.3 | 5 | 18.0 | 3.15 (.4) | -338.5 |
| 3 | 0.05 | 1.25 | 0.2 | 5 | 12.0 | 1.5 (.7) | -399.0 |
| 4 | 0.05 | 0.833 | 0.1 | 1.667 | 18.0 | 2.6 (.6) | -340.6 |
| 3 | 0.05 | 1.25 | 0.0667 | 1.667 | 12.1 | 4.85 (1.0) | -429.0 |

Table 5.5: Measurements of the input impedance of a vertical monopole over an imperfect ground at Waldorf, MD. The measurements were taken using an HP4195 Network Analyzer in the Network Configuration. The variation in resistance values are shown in parenthesis.

| Ant. # | Ant. height (λ) | Ant. height (m) | Screen radius (λ) | Screen radius (m) | Frequency (MHz) | $\Delta Z = Z_{imp.} - Z_{perf.}$ ΔR | ΔX |
|---|---|---|---|---|---|---|---|
| 2 | 0.1 | 1.667 | 0.3 | 5 | 18.0 | 0.06 | 9.4 |
| 1 | 0.1 | 2.5 | 0.2 | 5 | 12.0 | -0.75 | 3.3 |
| 2 | 0.1 | 1.667 | 0.1 | 1.667 | 18.0 | 1.26 | -30.8 |
| 1 | 0.1 | 2.5 | 0.0667 | 1.667 | 12.1 | 2.1 | 3.0 |
| 4 | 0.05 | 0.833 | 0.3 | 5 | 18.0 | -0.25 | 2.3 |
| 3 | 0.05 | 1.25 | 0.2 | 5 | 12.0 | -2.2 | 39.9 |
| 4 | 0.05 | 0.833 | 0.1 | 1.667 | 18.0 | -0.8 | 0.2 |
| 3 | 0.05 | 1.25 | 0.0667 | 1.667 | 12.1 | 1.15 | 9.9 |

Table 5.6: The change in the measured input impedance from a vertical monopole over an imperfect ground to the same antenna over a perfect ground. Waldorf measurements were taken using an HP4195 Network Analyzer in the Network Configuration, whereas measurements taken at Brandywine used an HP4195 in the Impedance configuration.

| Ant. # | Ant. height (λ) | Ant. height (m) | Screen radius (λ) | Screen radius (m) | Frequency (MHz) | $\Delta Z = Z_{imp.} - Z_{perf.}$ ΔR | ΔX |
|---|---|---|---|---|---|---|---|
| 2 | 0.1 | 1.667 | 0.3 | 5 | 18.0 | 1.049 | 1.535 |
| 1 | 0.1 | 2.5 | 0.2 | 5 | 12.0 | 1.136 | 1.316 |
| 2 | 0.1 | 1.667 | 0.1 | 1.667 | 18.0 | 2.554 | 0.344 |
| 1 | 0.1 | 2.5 | 0.0667 | 1.667 | 12.0 | 4.256 | 0.541 |
| 4 | 0.05 | 0.833 | 0.3 | 5 | 18.0 | 0.316 | 0.640 |
| 3 | 0.05 | 1.25 | 0.2 | 5 | 12.0 | 0.348 | 0.693 |
| 4 | 0.05 | 0.833 | 0.1 | 1.667 | 18.0 | 0.741 | 0.337 |
| 3 | 0.05 | 1.25 | 0.0667 | 1.667 | 12.0 | 1.315 | 0.497 |

Table 5.7: The change in the input impedance from a vertical monopole over an imperfect ground to the same antenna over a perfect ground, as calculated from expressions in Section II using Mathematica®.

Regarding the values for $\Delta R$ in Tables 5.6 and 5.7, the measurements are too varied to provide any correlation or verification of the theory, although they are close in magnitude. With the variation in the measurements of the antenna systems at Waldorf ranging from +/- 0.25 to +/- 1.0 $\Omega$, the relative similarity between the $\Delta R$ values in both tables (+/- 2.1 in the worst case) is slightly supportive of the computational method.

The calculated $\Delta X$ vs. experimental $\Delta X$ showed almost no correlation between theory and measurements. One should note that the ground conditions for Waldorf on 8/3/90 did not meet the criteria (equation (2.5), Section II) for application of the theory to this problem. Due to the correlation between the predicted NEC values for the input impedance of the four monopoles over perfect ground and the measured values of the same antennas at Brandywine, one suspects (as in Section IV) that the predicted $\Delta X$ is affected detrimentally by the poor ground conditions. The discrepancy between the required and acutal ground conductivity for the theory are believed to be a significant cause of the poor correlation between the theoretical and experimental results for $\Delta X$.

It should also be noted that the field site selected at Waldorf had metal structures (as well as the measurement equipment) within 2 wavelengths of the antenna being tested. Although the electrical height of the antennas were quite short, there may have been some effects from coupling to these extraneous conductors. It should be noted that the same test bed configuration (antennas, base, coaxial cable and network analyzer) performed quite close to theoretical predictions at the Brandywine site, where there were no extraneous structures or equipment even close to the antennas being tested.

## VI. Conclusions

It was determined that the equations for the input impedance of a vertical monopole provided by Wait are rather strictly limited to the "good" ground case, i.e., ground with a high conductivity. It was determined by experiment that a good ground rarely occurs in areas near to the Potomac River, in Virginia or Maryland.

The following guidelines for using a ground screen for a vertical monopole are presented below:

1) A practical radial length is $0.3\lambda$ for monopoles less than $\lambda/4$ in height, as suggested by Figures 3.3a and 3.3b. In general, the radial length should exceed the monopole height.
2) The number of radials can have a profound effect on $\Delta R$, $\Delta X$ when the ground is poor (i.e., low conductivity). In general, using the largest number of radials possible is recommended, although one suffers diminishing returns after 200 radials.
3) If the ground constants do not meet the criteria in equation (2.5), the expressions in Section II will not apply. A ground screen is even more essential for the case of a "poor" ground.

Although not illustrated in this report, it has been demonstrated [5] that increasing wire radius contributes little to the effectiveness of the ground system.

Impedance measurements at HF were made difficult by ground imperfections and a crowded electromagnetic environment, coupled with an input impedance with a phase approximating $90^{o}$ (inherent to vertical monopoles off resonance). Future investigation is suggested to develop a theorectical expression for Z that does not require such a high ground conductivity. Comparisons could then be made with data herein and with NEC model predictions.

## VII. References


1. Blake, L.V., Antennas, Artech House, Inc.,1986.

2. Sommerfeld, Arnold, "Partial Differential Equations in Physics", Lectures on Theoretical Physics, Vol. VI, Acedemic Press, Inc., 1949, Ch. VI.

3. Wait, J.R. and W.A. Pope, "The Characteristics of a Vertical Antenna with a Radial Conductor Ground System," Applied Sci. Res., Section B, Vol. 4, pp. 177-195, 1954.

4. MacFarlane, G.G., Journal of Institute of Electrical Engineers, Vol.93, Part IIIA, 1946, pp.1523

5. Maley, S.W., King, R.J., and L.R. Branch,"Theoretical Calculations of the Impedance of a Monopole Antenna with a Radial-Wire Ground System on an Imperfectly Conducting Half-Space," AF Cambridge Research Lab., AFCRL-63-583, Report No. 26, 13 December 1963.

6. © 1991 Wolfram Research, Inc. *Mathematica* is a registered trademark of Wolfram Research, Inc.

7. G.J. Burke, et al., "Numerical Electromagnetics Code (NEC) - Method of Moments", Lawrence Livermore National Laboratory, UCID-18834.

7. Li, Shing Ted, et al,"Microcomputer Tools for Communications Engineering," Artech House, Inc., pp. 177, Table 16-1.

8. Rupar, Michael, A.,"Computations and Measurements of the Input Impedance of a Vertical Monopole over Perfect and Imperfect Ground," Master's Thesis, The George Washington University, January 1991.

9. Collin, Zucker, "Antenna Theory," Vol.2, Chapter 23 by James, R. Wait.

10. Gilchrist, Dr. R.B., "HARDENDED ANTENNA TECHNOLOGY: Antenna Engineering Design Hanbook for Buried Linear Arrays," Vol. II, RADC-TR-89-54, May 1989.

11. Smith, G.S. and Norgard, J.D., "Measurement of the Electrical Constitutive Parameters of Materials Using Antennas," IEEE Transactions on Antennas and Propagation, July 1985, p. 783.

## Appendix A:
## Theoretical Development of the Impedance of a Monopole due to the Presence of a Lossy Ground.

The following derivation of the input impedance of a vertical monopole over an imperfect ground parallels the original work done on this subject by Wait and Pope [3]. The effects of top loading are treated simply as an increase in the height of the monopole.

The theoretical development of an expression for the impedance of a vertical monopole begins with Maxwell's Equations. The Hertz Vector Potential $\vec{\Pi}$ is used to derive the general radiated field expressions. This Hertz Vector Potential was used in this capacity by Wait and Pope [3] and earlier by Sommerfeld [2]. The short dipole Hertz vector is the basis for our potential expression, and the vertical monopole is treated as the superposition of these dipoles. The expressions derived for the input impedance of a vertical monopole are evaluated numerically in Section III.

### 1. Background

Introduction of the Hertz Vector Potential

In the following, we develop the wave equation for the Hertz Vector Potential (also referred to as simply the Hertz Potential) and its solution. Note that this derivation is for isotropic, homogeneous media.

It was shown by Hertz that one can define an electromagnetic field in terms of a single vector potential function when the currents satisfy the law of conservation of charge. This function, the Hertz Potential, $\vec{\Pi}$, can be used to obtain the general vector and scalar potentials with the following relations:

$$\vec{A} = \frac{1}{c^2}\frac{\partial \vec{\Pi}}{\partial t} \qquad \text{(A.1.1a)}$$

$$\phi = -\nabla \bullet \vec{\Pi} \qquad \text{(A.1.1b)}$$

Faraday's Law is then used to define the electric field vector $\vec{E}$:

$$\nabla \times \vec{E} = -\frac{\partial \vec{B}}{\partial t} = -\frac{\partial}{\partial t}(\nabla \times \vec{A})$$

$$\nabla \times (\vec{E} + \frac{\partial \vec{A}}{\partial t}) = 0$$

Since $\nabla \times \nabla\phi = 0$, one may state that:

$$\vec{E} + \frac{\partial \vec{A}}{\partial t} = -\nabla\phi$$

An expression for $\vec{E}$ is found using (A.1.1a) and (A.1.1b):

$$\vec{E} = \nabla(\nabla \bullet \vec{\Pi}) - \frac{1}{c^2}\frac{\partial^2 \vec{\Pi}}{\partial t^2} \qquad \text{(A.1.2)}$$

The magnetic field, $\vec{H}$, can also be expressed in terms of the Hertz Potential:

$$\mu\vec{H} = \nabla \times \vec{A}$$

$$\vec{H} = \frac{1}{\mu}\nabla \times \frac{1}{c^2}\frac{\partial \vec{\Pi}}{\partial t}$$

$$\vec{H} = \varepsilon\frac{\partial}{\partial t}(\nabla \times \vec{\Pi}) \qquad \text{(A.1.3)}$$

The expressions in (A.1.2) and (A.1.3) are substituted into the following expression from Maxwell's equations (for a source-free region):

$$\nabla \times \vec{H} - \frac{\partial \vec{D}}{\partial t} = 0 \qquad \text{(A.1.4)}$$

where $\vec{D}$ is the electric flux density, $\vec{D} = \varepsilon\vec{E}$.

$$\nabla \times \varepsilon\frac{\partial}{\partial t}(\nabla \times \vec{\Pi}) - \varepsilon\frac{\partial}{\partial t}\left[\nabla(\nabla \bullet \vec{\Pi}) - \frac{1}{c^2}\frac{\partial^2\vec{\Pi}}{\partial t^2}\right] = 0$$

$$\frac{\partial}{\partial t}\left[\nabla \times \nabla \times \vec{\Pi} - \nabla(\nabla \bullet \vec{\Pi}) + \frac{1}{c^2}\frac{\partial^2\vec{\Pi}}{\partial t^2}\right] = 0$$

which, after integrating, gives the expression:

$$\nabla \times \nabla \times \vec{\Pi} - \nabla(\nabla \bullet \vec{\Pi}) + \frac{1}{c^2}\frac{\partial^2\vec{\Pi}}{\partial t^2} = \begin{array}{l}\text{constant function}\\ \text{of the space}\\ \text{coordinates}\end{array} \qquad \text{(A.1.5)}$$

The value of the constant makes no difference in the determination of the field term, so it is set equal to zero.

Using the vector identity $\nabla^2\vec{\Pi} = \nabla(\nabla \bullet \vec{\Pi}) - \nabla \times \nabla \times \vec{\Pi}$, (A.1.5) becomes

$$\nabla^2\vec{\Pi} - \frac{1}{c^2}\frac{\partial^2\vec{\Pi}}{\partial t^2} = 0 \qquad \text{(A.1.6)}$$

which is the wave equation for the Hertz vector. With an assumed time dependance of $e^{j\omega t}$ and operating in the spherical coordinate system, (A.1.6) can be reduced to

$$(\nabla^2 - \gamma^2)\vec{\Pi} = 0 \qquad (r \neq 0) \qquad \text{(A.1.7)}$$

where:

$$\frac{\omega^2}{c^2} = k^2 = -\gamma^2$$

and $\gamma$ is Wait's notation for the propagation constant [3]. The solution for the Hertz Potential $\vec{\Pi}$ in the general spherical wave case (with a unit, $\hat{z}$ polarized, dipole moment source at the origin) is:

$$\vec{\Pi} = \frac{1}{4\pi r} e^{-j(kr - \omega t)} \hat{z} \qquad \text{(A.1.8)}$$

In the derivation that follows, the Hertz Potential is defined using the convention of a positive phase term,

$$\vec{\Pi} = \frac{1}{4\pi r} e^{j(kr - \omega t)} \hat{z} \qquad \text{(A.1.9)}$$

which results in slightly different expressions for reactances. Equation (A.1.9) was used to keep the derivation as close as possible to the work done by Sommerfeld. When returning to Wait's development, and when referring to the input reactance of an antenna in later sections, the convention of a positive reactance being inductive and a negative reactance being capacitive will be used.

The Scalar Wave Equation for the Magnetic Field

Beginning with (A.1.5), (with the constant equal to zero), the curl of both sides is taken, and the vector $\vec{\beta} = \nabla \times \vec{\Pi}$ is introduced:

$$\nabla \times \nabla(\nabla \bullet \vec{\Pi}) - \nabla \times \nabla \times (\nabla \times \vec{\Pi}) - \frac{1}{c^2} \nabla \times \frac{\partial^2 \vec{\Pi}}{\partial t^2} = 0$$

For any scalar function $\phi$, $\nabla \times \nabla\phi = 0$. Therefore, the first term drops out of the above expression. Taking the second time derivative in the last term:

$$0 - \nabla \times \nabla \times \vec{\beta} - \gamma^2 \vec{\beta} = 0$$

$$- \nabla(\nabla \bullet \vec{\beta}) + \nabla^2 \vec{\beta} - \gamma^2 \vec{\beta} = 0$$

Since the divergence of a curl equals zero, the first term drops out, leaving:

$$\nabla^2\vec{\beta} - \gamma^2\vec{\beta} = 0 \qquad \text{(A.1.10)}$$

Taking the time derivative of both sides and dividing through by $\mu c^2$, (A.1.10) becomes:

$$\frac{1}{\mu c^2}\frac{\partial}{\partial t}(\nabla^2\vec{\beta}) - \frac{1}{\mu c^2}\frac{\partial}{\partial t}(\gamma^2\vec{\beta}) = 0$$

$$\nabla^2[\frac{1}{\mu c^2}\frac{\partial}{\partial t}(\nabla\times\vec{\Pi})] - \gamma^2[\frac{1}{\mu c^2}\frac{\partial}{\partial t}(\nabla\times\vec{\Pi})] = 0$$

$$\nabla^2\vec{H} - \gamma^2\vec{H} = 0 \qquad \text{(A.1.11)}$$

In order to parallel the work done by Wait [3], equation (A.1.11) needs to be reduced to the form of a scalar wave equation. Such an expression can be derived for the particular case of the vertical monopole. The Hertz field for a vertical monopole can be written as $\vec{\Pi} = \Pi_z\,\hat{z}$. Converting to the equivalent magnetic field expression, one finds that $\vec{H} = H_\phi\,\hat{\phi}$. Utilizing cylindrical symmetry, one may further assume that $\vec{H} = H_\phi(\rho,z)\,\hat{\phi}$. Therefore, (A.1.11) may be developed as follows:

$$\nabla(\nabla\bullet\vec{H}) - \nabla\times\nabla\times\vec{H} - \gamma^2\vec{H} = 0$$

$$\nabla\bullet\vec{H} = \frac{1}{\rho}\frac{\partial H_\phi}{\partial\phi} = \frac{1}{\rho}\frac{\partial}{\partial\phi}(H_\phi(\rho,z)) = 0 \qquad \text{(A.1.12)}$$

$$\nabla\times H_\phi\,\hat{\phi} = -\frac{\partial H_\phi}{\partial z}\,\hat{\rho} + \frac{1}{\rho}\frac{\partial}{\partial\rho}(\rho\,H_\phi)\,\hat{z}$$

$$= -\frac{\partial H_\phi}{\partial z}\,\hat{\rho} + \frac{1}{\rho}(H_\phi + \rho\frac{\partial H_\phi}{\partial\rho})\,\hat{z}$$

$$\nabla\times\nabla\times H_\phi\,\hat{\phi} = -\hat{\phi}\,[\frac{\partial}{\partial\rho}(\frac{H_\phi}{\rho} + \frac{\partial H_\phi}{\partial\rho}) + \frac{\partial^2 H_\phi}{\partial z^2}]$$

$$= -\hat{\phi}\left[\frac{\partial^2 H_\phi}{\partial \rho^2} + \frac{\partial}{\partial \rho}\left(\frac{1}{\rho} H_\phi\right) + \frac{\partial^2 H_\phi}{\partial z^2}\right] \qquad \text{(A.1.13)}$$

Substituting (A.1.12) and (A.1.13) into (A.1.11), one obtains the following:

$$\nabla^2 \vec{H} - \gamma^2 \vec{H} = -\nabla \times \nabla \times H_\phi \hat{\phi} - \gamma^2 H_\phi \hat{\phi}$$

$$= \hat{\phi}\left[\frac{\partial^2 H_\phi}{\partial \rho^2} + \frac{\partial}{\partial \rho}\left(\frac{1}{\rho} H_\phi\right) + \frac{\partial^2 H_\phi}{\partial z^2} - \gamma^2 H_\phi\right]$$

$$= \left[\frac{1}{\rho}\frac{\partial}{\partial \rho}\left(\rho \frac{\partial H_\phi}{\partial \rho}\right) + \frac{\partial^2 H_\phi}{\partial z^2} - \gamma^2 H_\phi\right]\hat{\phi} = 0 \qquad \text{(A.1.14)}$$

Since $H_\phi$ is not a function of ø, one may add the term $\frac{1}{\rho^2}\frac{\partial^2 H_\phi}{\partial \phi^2}\hat{\phi}$ to (A.1.14), which reduces it to the desired scalar wave equation:

$$\nabla^2 H_\phi - \gamma^2 H_\phi = 0 \qquad \text{(A.1.15)}$$

Note that equation (A.1.15) is not satisfied by Hø in the general case when Hø is dependent on ø.

## 2. Determining the Input Impedance for a Vertical Monopole

This follows the method for obtaining the input impedance of a vertical monopole over an imperfect ground used by Wait [3].

The development begins with a simple vertical antenna element along the z-axis of height h, situated above a ground half-space, as shown in Figure A.2.1.

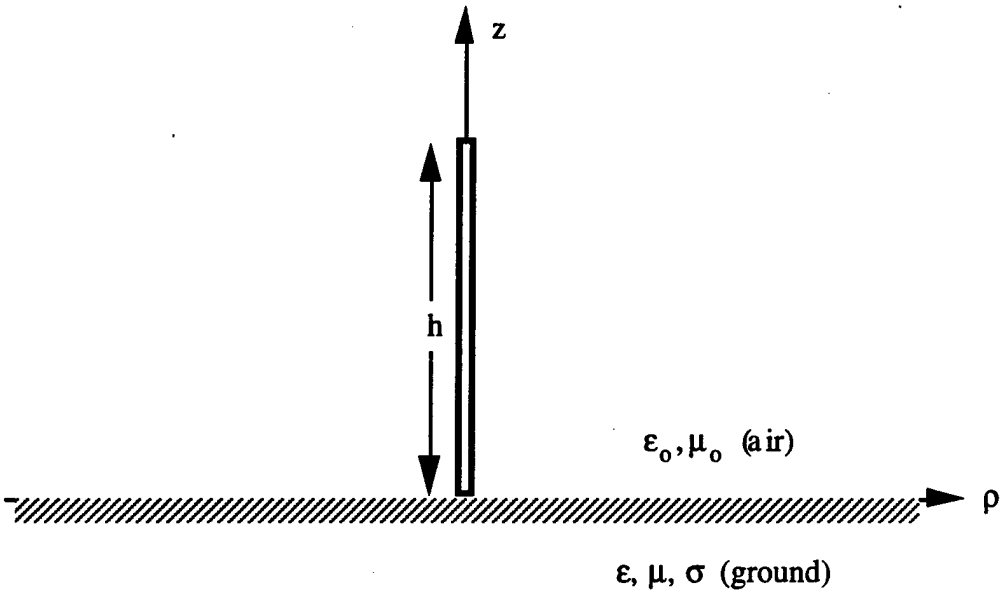


Figure A.2.1: The representation of a vertical monopole over an imperfect ground. The monopole is just above the ground plane.

The propagation constant ($\gamma$) and the characteristic impedance ($\eta$) of the imperfect ground are given as:

$$\gamma = \sqrt{j\omega\mu(\sigma + j\omega\varepsilon)}$$

$$\eta = \sqrt{\frac{j\omega\mu}{j\omega\varepsilon + \sigma}}$$

For free space (and air), these two quantities are defined as:

$$\gamma_o = j\omega\sqrt{\mu\varepsilon_o} \equiv j\beta = j\,\frac{2\pi}{\lambda}$$

$$\eta_o = \sqrt{\frac{\mu_o}{\varepsilon_o}}$$

Note that $\mu = \mu_o$ is assumed throughout this paper, which is the case for normal soil with little inherent magnetization.

The antenna's self-impedance is separated into two parts,

$$Z_T = Z_O + \Delta Z_T \qquad \text{(A.2.1)}$$

where $Z_T$ is the total input impedance, and $Z_O$ is the input impedance of the same antenna over a perfect ground. $\Delta Z_T$ represents the difference between the perfect and imperfect ground scenarios. One may think of the perfect ground case as an infinite ground screen.

Wait's paper focused on the definition of $\Delta Z_T$ , and then applied this factor to both the lossy ground and the imperfect ground screen problems. The following is a detailed outline of that development, using information from Sommerfeld [2] to complete some involved portions of the mathematics.

The total flux emanating from a cylindrical surface surrounding the antenna is given as:

$$F = \int_S \vec{E} \times \vec{H} \bullet \hat{n}\, ds \qquad \text{(A.2.2)}$$

$$= -\lim_{\rho \to 0} 2\pi\rho \int_0^h E_z H_\phi \, dz$$

The limit $\rho \to 0$ is taken assuming the antenna is an infinitesimal vertical element, so that the only integration is over the sides of the imaginary cylinder, with $\hat{n} = \hat{\rho}$. The negative sign is included because the flux is assumed to be radiating outward.

An expression for $\vec{E}$ is taken from Maxwell's Equations:

$$\nabla \times \vec{H} = \frac{\gamma}{\eta} \vec{E}$$

$$E_Z = \frac{\eta}{\gamma} \left[\frac{1}{\rho} \frac{\partial}{\partial \rho} (\rho H_\phi)\right] \qquad \text{(A.2.3)}$$

The $H_\phi$ can be found using Ampere's law for a symmetrical cylindrical conductor (quasi-stationary case):

$$\int_C \vec{H} \cdot d\vec{L} = I$$

$$\int_0^{2\pi} H_\phi \rho \, d\phi = H_\phi \rho \int_0^{2\pi} d\phi = I$$

$$H_\phi = \frac{I}{2\pi\rho} \qquad \text{(A.2.4)}$$

Alternatively, $\hat{n} \times (\vec{H}_2 - \vec{H}_1) = \vec{J}_s$ leads to the same result.

Using (A.2.3), (A.2.4) and Ohm's Law, one gets an expression for the input impedance Z:

$$Z = \frac{F}{I_o^2} = -\frac{1}{I_o^2} \lim_{\rho \to 0} \int_0^h E_Z \, I(z) \, dz \qquad \text{(A.2.5)}$$

The electric field can be expressed as $E_z = E_z^\infty + E_z^s$, with $E_z^\infty$ being the electric field over a perfect ground and $E_z^s$ being the change in the field which accounts for the effects of the imperfect ground and ground system. Therefore, using equations (A.2.1) - (A.2.5), one may express the input impedance increment $\Delta Z_T$ as:

$$\Delta Z_T = \left[ -\frac{1}{I_o^2} \int_0^h E_z^s \, I(z) \, dz \right]_{\lim_{\rho \to 0}}$$

$$\Delta Z_T = \left[ -\frac{\eta_o}{\gamma_o I_o^2} \int_0^h \left\{ \frac{1}{\rho} \frac{\partial}{\partial \rho} (\rho \, H_\phi^s) \right\} I(z) \, dz \right]_{\lim_{\rho \to 0}} \qquad \text{(A.2.6)}$$

The values $\eta_o$ and $\gamma_o$ are used because the integration takes place in free space, and any ground effects on the antenna impedance are incorporated into the $H_\phi^s$ term.

To obtain $H_{\phi}^{s}$, one first solves the wave equation for the Hertz potential, then converts that solution to the magnetic field expression desired. The solution is taken from Sommerfeld [2], whose solution assumed a potential of $\vec{\Pi}\,\hat{z}$ (written as $\Pi_z$) for a vertical dipole along the z-axis. The Hertz wave equation from equation (A.2.7) is:

$$\nabla^2\Pi_z + k^2\Pi_z = 0 \qquad (r \neq 0) \qquad \text{(A.2.7)}$$

where $ik = \gamma$, or $-k^2 = \gamma^2$. The derivation of the primary (radiated) field is begun by representing the solution of (A.2.7) as a superposition of eigenfunctions (u) with eigenvalues ($\lambda$). Incorporating the cylindrical symmetry of the vertical monopole problem, the eigenfunctions will take the form of Bessel functions, with the index n = 0. The general field solution for a cylinder of height h is:

$$u_{nm} = I_n(\lambda r)\, e^{jn\phi} \cos\frac{m\pi z}{h} \qquad m,n \in \text{integers}$$

$$u_m = I_o(\lambda r) \cos\frac{m\pi z}{h}$$

Here, r is used instead of $\rho$ as the radial component, to be consistent with Sommerfeld's notation. Once an expression for $\Pi_z$ is obtained, the derivation reverts to the original notation used by Wait [3]. Sommerfeld then replaces the index $m\pi/h$ with $\mu$ (which has no relation to the permeability), and the solution of (A.2.7) becomes:

$$u_m = I_o(\lambda r) \cos \hat{\mu} z \quad \text{where } \hat{\mu} = \sqrt{k^2 - \lambda^2} \qquad \text{(A.2.8)}$$

The cosine function meets the boundary conditions for the top and bottom of a circular cylinder. However, for the development of a vertical monopole solution, there is no such boundary condition on the upper half plane, so one can replace the cosine function with an exponential:

$$u_m = I_o(\lambda r)\, e^{-\mu z} \quad \text{where } \mu = \sqrt{\lambda^2 - k^2} \qquad \text{(A.2.9)}$$

The expression for $\mu$ is found by substituting $u_m$ into (A.2.7) for $\Pi_z$. Since the vertical monopole is assumed to only produce the Hertz field along the z-axis, the expression for $\Pi_z$ encompasses the entire solution, and can be referred to as $\Pi$. From (A.2.8) and (A.2.9), the solution for $\Pi$ takes the form:

$$\Pi = \int_0^\infty F(\lambda)\, I_o(\lambda r)\, e^{-\mu z}\, d\lambda \quad (z < 0) \tag{A.2.10}$$

The solution is expressed as an integral combination of eigenfunctions because of the infinite number of eigenvalues present when dealing with an unbounded case, such as the upper half plane.

To solve for the coefficient $F(\lambda)$, one sets (A.2.10) equal to the spherical wave expression (in cylindrical coordinates) for the unit Hertz dipole potential below (Note: Sommerfeld assumed that the factor $1/4\pi$ was accounted for through the choice of units):

$$\Pi = \frac{e^{jkR}}{R} \qquad \text{where } R^2 = z^2 + r^2 \tag{A.2.11}$$

Setting (A.2.10) and (A.2.11) equal and setting z equal to zero, one ends up with the boundary condition:

$$\frac{e^{jkr}}{r} = \int_0^\infty F(\lambda)\, I_o(\lambda r)\, d\lambda \tag{A.2.12}$$

Using the double Fourier integral expression (from [2], section 21B):

$$f(r) = \int_0^\infty \sigma \, d\sigma \int_0^\infty f(\rho) \, I_n(\sigma r) \, I_n(\sigma \rho) \, \rho \, d\rho$$

$$\text{or: } f(r) = \int_0^\infty \sigma \, d\sigma \, \phi(\sigma) \, I_n(\sigma r)$$

$$\text{with } \phi(\sigma) = \int_0^\infty \rho \, d\rho \, f(\rho) \, I_n(\sigma \rho)$$

Setting f(r) equal $\vec{\Pi}$:

$$f(r) = \int_0^\infty \sigma \, d\sigma \, \phi(\sigma) \, I_n(\sigma r) = \int_0^\infty F(\lambda) \, I_o(\lambda r) \, d\lambda = \frac{e^{jkr}}{r}$$

$$\phi(\sigma) = \int_0^\infty \rho \, d\rho \, f(\rho) \, I_o(\sigma \rho)$$

$$= \int_0^\infty \rho \, d\rho \, \frac{e^{ik\rho}}{\rho} \, I_o(\sigma \rho)$$

so

$$f(r) = \int_0^\infty \sigma \, d\sigma \, \{ \int_0^\infty e^{ik\rho} \, I_o(\sigma \rho) \, d\rho \} \, I_o(\sigma r)$$

Let $\sigma = \lambda$:

$$f(r) = \int_0^\infty \lambda \, d\lambda \, \{ \int_0^\infty e^{jk\rho} \, I_o(\lambda \rho) \, d\lambda \} \, I_o(\lambda r) = \int_0^\infty F(\lambda) \, I_o(\lambda r) \, d\lambda$$

Therefore, $F(\lambda) = \lambda \, \phi(\lambda)$, and:

$$F(\lambda) = \lambda \int_0^\infty e^{jkr} \, I_o(\lambda r) \, dr \qquad \text{(A.2.13)}$$

To complete the solution for $F(\lambda)$, we use the explicit integral expression for the Bessel function ([2], equation 19.14):

$$I_n(r) = \frac{1}{2\pi} \int_{Wo} e^{jr\ \cos w}\, e^{jn(w\ -\ \pi/2)}\, dw$$

$$I_o(r) = \frac{1}{2\pi} \int_{-\pi}^{\pi} e^{jr\ \cos w}\, dw \qquad w \in \text{Real}$$

Substituting the variable $\lambda r$ for r in the above expression for n=0, this is then substituted into (A.2.13) to give:

$$F(\lambda) = \lambda \int_0^{\infty} e^{jkr} \frac{1}{2\pi} \int_{-\pi}^{\pi} e^{j\lambda r\ \cos w}\, dw\, dr$$

$$F(\lambda) = \frac{\lambda}{2\pi} \int_{-\pi}^{\pi} dw \int_0^{\infty} e^{jr\ (k\ +\ \lambda\ \cos w)}\, dr$$

$$= -\frac{\lambda}{j2\pi} \int_{-\pi}^{\pi} \frac{dw}{k + \lambda \cos w} \qquad \text{(A.2.14)}$$

The solution for this integral can be found using the following identity:

$$\int \frac{dx}{a + b\cos x} = \frac{2}{\sqrt{a^2 - b^2}} \tan^{-1} \left\{ \frac{(a - b) \tan\left(\frac{x}{2}\right)}{\sqrt{a^2 - b^2}} \right\} \qquad [a^2 > b^2]$$

which requires that $k^2 > \lambda^2$. Requiring $\mu$ to be complex with a positive real part, we can see from its original definition in (A.2.8) that $k^2$ must be greater than $\lambda^2$. The solution for $F(\lambda)$ is:

$$F(\lambda) = \frac{-\lambda}{j\sqrt{k^2 - \lambda^2}} = \frac{\lambda}{\mu}; \qquad \text{where } \mu = \sqrt{\lambda^2 - k^2} \qquad \text{(A.2.15)}$$

From (A.2.15) and (A.2.10), the solution for the Hertz Potential is found to be:

$$\Pi = \int_0^\infty I_o(\lambda r)\, e^{-\mu z} \frac{\lambda}{\mu}\, d\lambda \qquad \text{(A.2.16)}$$

Using equations (A.2.3) and (A.2.9) (and substituting the notation of J for I for the Bessel function), one may use the above expression to develop the eigenfunction solution to the wave equation for the tangential magnetic field:

$$H_\phi^s\ (r,z) = \int_0^\infty J_1(\lambda r)\, e^{-\mu z}\, f(\lambda)\, \lambda\, d\lambda \qquad z \geq 0$$

where $f(\lambda)$ takes into account the secondary (reflected) field, the $1/\mu(\lambda)$ term, and the constants that result from converting $\Pi$ to $H_\phi$. The $H_\phi$ term represents the change in the radiated tangential magnetic field due to the finite conductivity of the earth (and the ground system, if any).

Converting $H_\phi$ to Wait's notation, a time dependance of $e^{+j\omega t}$ is assumed, and one replaces $\lambda r$ with $\lambda\rho$ and $k^2$ with $-\gamma^2$. Since we are dealing with the upper half plane (air medium), we replace $\mu$ with $\mu_o$, where $\mu_o$ is defined as $\mu_o = (\lambda^2 + \gamma_o^2)^{1/2}$. Utilizing Wait's notation produces the following expression:

$$H_\phi^s(\rho,z) = \int_0^\infty J_1(\lambda\rho)\, e^{-\mu_o z}\, f(\lambda)\, \lambda\, d\lambda \qquad (z \geq 0) \qquad \text{(A.2.17)}$$

which is identical to equation (35) in [3]. Recall that for this development only, $\mu_o$, like $\mu$, is an index, and not the permeability of the ground. From (A.2.17), one may find the electric field tangent to the ground plane:

$$E_\rho(\rho,0) = -\frac{\eta}{\gamma}\frac{\partial H_\phi}{\partial z}\Big|_{z=0} = -\frac{\eta_o}{\gamma_o}\int_0^\infty J_1(\lambda\rho)\, f(\lambda)\, \mu_o\, \lambda\, d\lambda \qquad \text{(A.2.18)}$$

where $f(\lambda)$ is defined by the inverse Fourier relation:

$$f(\lambda) = -\frac{\gamma_o}{\eta_o \mu_o} \int_0^\infty J_1(\lambda\rho')\, E_\rho(\rho',0)\, \rho'\, d\rho'$$

Substituting $f(\lambda)$ back into (A.2.17) results in the following expression:

$$H_\phi^s(\rho,z) = \int_0^\infty J_1(\lambda\rho)\, e^{-\mu_o z} \left\{ -\frac{\gamma_o}{\eta_o \mu_o} \int_0^\infty J_1(\lambda\rho')\, E_\rho(\rho',0)\, \rho' d\rho' \right\} \lambda d\lambda \qquad \text{(A.2.19)}$$

This expression is then substituted into (A.2.5), with $\Delta Z_T$ hereafter referred to as $\Delta Z$:

$$\Delta Z = -\frac{1}{I_o^2} \int_0^h \left[ \int_0^\infty \int_0^\infty \lim_{\rho\to 0} \left\{ \frac{1}{\rho} \frac{\partial}{\partial\rho} \rho J_1(\lambda\rho)\, e^{-\mu_o z} \frac{\lambda}{\mu_o} d\lambda \right\} J_1(\lambda\rho') E_\rho(\rho',0) \rho' d\rho' \right] I(z)\, dz$$

Using the recursion relations for the Bessel function:

$$\frac{\partial}{\partial\rho} J_1(\lambda\rho) = \lambda \left( -\frac{1}{\lambda\rho} J_1(\lambda\rho) + J_o(\lambda\rho) \right)$$

$$\begin{aligned} \frac{\partial}{\partial\rho} \rho J_1(\lambda\rho) &= \rho \frac{\partial J_1(\lambda\rho)}{\partial\rho} + J_1(\lambda\rho) \\ &= \rho \{ -\frac{1}{\rho} J_1(\lambda\rho) + \lambda J_o(\lambda\rho) \} + J_1(\lambda\rho) \\ &= \lambda\rho\, J_o(\lambda\rho) \end{aligned}$$

$$\lim_{\rho\to 0} \frac{1}{\rho} \left[ \frac{\partial}{\partial\rho} (\rho\, J_1(\lambda\rho)) \right] = \lim_{\rho\to 0} \frac{\lambda\rho J_o(\lambda\rho)}{\rho} = \lambda$$

$\Delta Z$ is rewritten as:

$$\Delta Z = -\frac{1}{I_o^2} \int_0^h \left[ \int_0^\infty \int_0^\infty e^{-\mu_o z} \frac{\lambda^2}{\mu_o} d\lambda\; J_1(\lambda\rho')\, E_\rho(\rho',0)\, \rho' d\rho' \right] I(z) dz \qquad \text{(A.2.20)}$$

Using:

$$J_1(\lambda\rho') = -\frac{1}{\lambda}\frac{\partial J_o(\lambda\rho')}{\partial\rho'}$$

and Sommerfeld's integral expression:

$$\int_0^\infty e^{-\mu_o z}\frac{\lambda}{\mu_o}\,J_o(\lambda\rho)\,d\lambda = \frac{e^{-\gamma_o\sqrt{z^2+\rho^2}}}{\sqrt{z^2+\rho^2}}$$

equation (A.2.20) is reduced as follows:

$$\Delta Z = -\frac{1}{I_o^2}\int_0^h\int_0^\infty -\frac{\partial}{\partial\rho'}\left[\int_0^\infty J_o(\lambda\rho')\,e^{-\mu_o z}\frac{\lambda}{\mu_o}\,d\lambda\right] E_\rho(\rho',0)\rho'd\rho' I(z)dz$$

$$= \frac{1}{I_o^2}\int_0^h\int_0^\infty \frac{\partial}{\partial\rho}\frac{e^{-\gamma_o(z^2+\rho^2)^{1/2}}}{\sqrt{z^2+\rho^2}}\,E_\rho(\rho,0)\,\rho\,d\rho\,I(z)\,dz$$

$$= -\frac{1}{I_o^2}\int_0^h(-1)\int_0^\infty \frac{\partial}{\partial\rho}\frac{e^{-\gamma_o(z^2+\rho^2)^{1/2}}}{\sqrt{z^2+\rho^2}}\,E_\rho(\rho,0)\,\frac{2\pi\rho}{2\pi}\,d\rho\,I(z)\,dz$$

$$\Delta Z = -\frac{1}{I_o^2}\int_0^\infty H_\phi^\infty(\rho,0)\,E_\rho(\rho,0)\,2\pi\rho\,d\rho \qquad \text{(A.2.21a)}$$

where $H_\phi^\infty(\rho,0)$ is the tangential magnetic field at the boundary for a perfect ground plane:

$$H_\phi^\infty(\rho,0) = -\frac{1}{2\pi}\int_0^h \frac{\partial}{\partial\rho}\left[\frac{e^{-\gamma_o(z^2+\rho^2)^{1/2}}}{\sqrt{z^2+\rho^2}}\right] I(z)\,dz \qquad \text{(A.2.21b)}$$

Equation (A.2.21b) can be found in [3] and [9], but no explanation is given. Note that the integrand of (A.2.21b) is quite similar to the basic field

expression for the Hertz potential (A.2.8), with the radial distance r being replaced by $(z^2 + \rho^2)^{1/2}$, and the entire term being weighted by the current over the length of the antenna. All ground effects are assumed to be incorporated into the $E\rho(\rho,0)$ term in (A.2.21a).

Heretofore, no assumptions have been made about the current on the antenna. The current is now assumed to be a sinusoidal distribution, with no variation with respect to $\rho$ (i.e., an infinitesimally thin antenna). Wait defines the current as:

$$I(z) = I_o \sin(\alpha - \beta z) / \sin\alpha$$

where $\alpha = \beta(h + h')$, h' being an additional height factor due to top loading. Integrating (A.2.21b) with the above current produces the following result:

$$H_{\varnothing}^{\infty}(\rho,0) = - \frac{jI_o}{2\pi \sin\alpha} \left[ \frac{e^{-j\beta r}}{\rho} \cos(\beta h - \alpha) - \frac{e^{-j\beta\rho}}{\rho} \cos\alpha - \frac{jh}{\rho} \frac{e^{-j\beta r}}{r} \sin(\alpha - \beta h) \right] \quad \text{(A.2.22)}$$

with $r = (z^2 + \rho^2)^{1/2}$.

The expression for the electric field in the earth surface is evaluated next, to establish the boundary conditions at the earth-air interface (z=0). The electric field near the surface takes a form similar to (A.2.18), with:

$$E_\rho(\rho,z) = - \frac{\eta}{\gamma} \int_0^{\infty} \mu J_1(\lambda\rho) e^{+\mu z} p(\lambda) \lambda d\lambda \quad ; z < 0$$

A binomial expansion is done on $\mu = (\lambda^2 + \gamma^2)^{1/2}$:

$$(a + x)^n = a^n + na^{n-1}x + \frac{n(n-1)a^{n-2}}{2!} x^2 + \ldots$$

$$\mu = \gamma\left[1 + \frac{\lambda^2}{2\gamma^2} + \frac{1}{8}\left(\frac{\lambda}{\gamma}\right)^4 + \ldots\right]$$

and the tangential electric field in the ground (z<0) becomes

$$E_\rho(\rho,z) = -\frac{\eta}{\gamma}\left[\int_0^\infty \gamma\, J_1(\lambda\rho) e^{\mu z} p(\lambda)\lambda d\lambda + \int_0^\infty \frac{1}{2\gamma} J_1(\lambda\rho) e^{\mu z} p(\lambda)\lambda^3 d\lambda + \ldots\right]$$

Since the Bessel functions are used in the solution, each function individually solves the wave equation:

$$(\nabla_\rho^2 - \lambda^2)\, J_o(\lambda\rho) = 0$$

$$\frac{\partial}{\partial\rho}\left(\frac{1}{\rho}\frac{\partial}{\partial\rho}\rho\frac{\partial J_o}{\partial\rho}\right) - \lambda^2\frac{\partial J_o}{\partial\rho} = 0$$

$$-\frac{\partial}{\partial\rho}\left(\frac{1}{\rho}\frac{\partial}{\partial\rho}\rho\, J_1(\lambda\rho)\right) = -\lambda^3 J_1(\lambda\rho)$$

Using the above expression, $E_\rho$ is simplified to:

$$E_\rho(\rho,z) = -\eta H_\phi - \frac{\eta}{2\gamma^2}\left(\frac{\partial}{\partial\rho}\frac{1}{\rho}\frac{\partial}{\partial\rho}\rho H_\phi\right) \pm \text{ H.O.T.} \qquad \text{(A.2.23a)}$$

with

$$H_\phi(\rho,z) = \int_0^\infty J_1(\lambda\rho)\, e^{\mu z}\, p(\lambda)\, \lambda\, d\lambda \;\; ; z \le 0 \qquad \text{(A.2.23b)}$$

which equals the total tangential H in the presence of the ground screen. ("H.O.T." is an acronym for higher order terms.)

In [3], Appendix II, Wait claimed that if the propagation constant $\gamma$ of the ground is large enough, and if $H_\phi$ varies slowly with respect to $\rho$, then only the first term of (A.2.23a) is significant. The first constraint is equivalent to requiring

that the ground displacement currents are an unimportant factor in the impedance calculation. At the surface, (A.2.23a) is reduced to:

$$E_\rho(\rho,0) = -\eta_c H_\phi(\rho,0) \qquad \text{(A.2.24)}$$

where $\eta_c$ represents the surface impedance of the air-ground interface. Wait also states that this simplification is valid when $|\gamma| >> \beta$, which is expressed as:

$$\left|\sqrt{j\mu\omega\sigma - \omega^2\mu\varepsilon}\right| >> \omega\sqrt{\mu_o\varepsilon_o} \qquad \text{(A)}$$

This can be reduced to:

$$\sqrt{\mu\omega}\sqrt[4]{\sigma^2 + \omega^2\varepsilon^2} >> \frac{\omega}{c}$$

Assuming a frequency of 18 MHz and a relative dielectric constant of 13 (based upon ground constant measurements made in the DC area and documented in Appendix B), condition (A) can be expressed as:

$$\sigma >> 0.0137$$

The requirement for a slowly varying Hø is determined by comparing the two coefficients from (A.2.23a):

$$\eta >> \frac{\eta}{2\gamma^2} \qquad \text{(B)}$$

which is equivalent to $|\gamma| >> \frac{1}{\sqrt{2}} = .7071$.

Condition B by itself could require a large conductivity, depending on the operating frequency. However, when Hø is limited to a slowly varying function, then the term $\frac{\partial}{\partial\rho}\frac{1}{\rho}\frac{\partial}{\partial\rho}\rho H_\phi$ is quite small, and the second term in equation (A.2.23a) may be deemed insignificant for normal values of ground conductivity and permittivity.

Recalling the expression for the change in impedance:

$$\Delta Z = -\frac{1}{I_o^2}\int_0^\infty H_\phi^\infty(\rho,0)\, E_\rho(\rho,0)\, 2\pi\rho\, d\rho \qquad \text{(A.2.21a)}$$

where $\Delta Z$ is the change in the input impedance of the antenna due to the influence of the imperfect ground. Using the approximation for $E\rho$ in (A.2.24), and assuming that $H_\phi^\infty(\rho,0)$ is equivalent to $H_\phi(\rho,0)$ in the region of the ground plane where $|M| >> \beta$, equation (A.2.21a) becomes:

$$I_o^2\,\Delta Z \cong \eta\int_0^\infty [H_\phi^\infty(\rho,0)]^2\, 2\pi\rho\, d\rho \qquad \text{(A.2.25)}$$

Substituting with the magnetic field expression (A.2.22), the current term ($I_o$) drops out, and (A.2.25) becomes:

$$\Delta Z = \int_0^\infty \frac{-\eta}{2\pi\sin^2\alpha}\Big[\frac{e^{-j2\beta r}}{\rho^2}\cos^2(\beta h-\alpha) - \frac{2e^{-j\beta(r+\rho)}}{\rho^2}\cos(\beta h-\alpha)\cos\alpha - \frac{2jhe^{-j2\beta r}}{r\rho^2}\cos(\beta h-\alpha)\sin(\alpha-\beta h) + \frac{e^{-j2\beta\rho}}{\rho^2}\cos^2\alpha + \frac{2jhe^{-j\beta(r+\rho)}}{r\rho^2}\sin(\alpha-\beta h)\cos\alpha - \frac{h^2e^{-j2\beta r}}{r^2\rho^2}\sin^2(\alpha-\beta h)\Big]\rho d\rho$$

$$\Delta Z = \frac{-\eta}{2\pi\sin^2\alpha}\Big\{\cos^2(\beta h-\alpha)\int_0^\infty\frac{e^{-j2\beta r}}{\rho}d\rho - 2\cos(\beta h-\alpha)\cos\alpha\int_0^\infty\frac{e^{-j\beta(r+\rho)}}{\rho}d\rho - 2jh\cos(\beta h-\alpha)\sin(\alpha-\beta h)\int_0^\infty\frac{e^{-j2\beta r}}{r\rho}d\rho + \cos^2\alpha\int_0^\infty\frac{e^{-j2\beta\rho}}{\rho}d\rho + 2jh\sin(\alpha-\beta h)\cos\alpha\int_0^\infty\frac{e^{-j\beta(r+\rho)}}{r\rho}d\rho - h^2\sin^2(\alpha-\beta h)\int_0^\infty\frac{e^{-j2\beta r}}{\rho r^2}d\rho \qquad \text{(A.2.26)}$$

For the case where there is no top loading, ($h' = 0$), $\alpha = \beta h$, and (A.2.26) is reduced to:

$$\Delta Z = \frac{-\eta}{2\pi \sin^2\beta h}\left[\int_0^\infty \frac{e^{-j2\beta r}}{\rho}\,d\rho - 2\cos\beta h\int_0^\infty \frac{e^{-j\beta(r+\rho)}}{\rho}\,d\rho - \cos^2\beta h\int_0^\infty \frac{e^{-j2\beta\rho}}{\rho}\,d\rho\right]$$

(A.2.27)

When calculating $\Delta Z$, the impedance term for the ground plane, $\eta$, can be factored out of the integrals. With $\rho$ in the denominator of each term, there is a singularity at $\rho$ equal to zero. Since the object is to calculate the change in impedance from a perfect to imperfect ground, one could say that a base plate made of a good conductor would not contribute to the expression for $\Delta Z$. Therefore, one can substitute the parameter "a" for the lower limit , where "a" is the radius of the "perfect" base.

In this report, equation (A.2.27) is used for computing $\Delta Z$, with the lower limit of integration changed to "a". To evaluate $\Delta Z$ in a non-integral form, one can use the exponential function Ei[-j$\beta$a]:

$$Ei[-j\beta a] = -\int_a^\infty \frac{e^{-j\beta\rho}}{\rho}\,d\rho = Ci(\beta a) + j\left[\frac{\pi}{2} - Si(\beta a)\right]$$

where Ci(x) and Si(x) are the cosine and sine integrals, respectively:

$$Ci(x) \equiv \int_\infty^x \frac{\cos t}{t}\,dt \qquad Si(x) \equiv \int_0^x \frac{\sin t}{t}\,dt$$

These are available as look-up tables, and are included in some mathematical software packages. Equation (A.2.27) and the exponential function can be combined to give the following non-integral expression $\Delta Z$:

$$\Delta Z = \frac{-\eta}{2\pi \sin^2\beta h}\{-\frac{1}{2}Ei[-j2\beta(r_o+h)]\,e^{j2\beta h} - \frac{1}{2}Ei[-j2\beta(r_o-h)]\,e^{-j2\beta h}$$
$$- 2\cos\beta h\left(-Ei[-j\beta(g+1)h]\,e^{j\beta h} - Ei[-j\beta(g-1)h]\,e^{-j\beta h} + Ei[-j\beta hg]\right)$$
$$+ \cos^2\beta h\,(Ei[-j2\beta a])\,\} \qquad \text{(A.2.28)}$$

where

$$r_o = (a^2 + h^2)^{1/2} \quad \text{and} \quad g = \frac{a + (a^2 + h^2)^{1/2}}{h}$$

Input Impedance for a Vertical Monopole Over a Radial Ground Screen

The inclusion of a radial ground screen at the base of the antenna has a significant effect on the impedance expression for the monopole. Although (A.2.28) still applies for the region beyond the ground screen ($\rho > a$), a separate expression must be formulated to account for the screen's effect on the surface magnetic and electric fields. The vertical monopole with a ground screen is shown in Figure A.2.2.

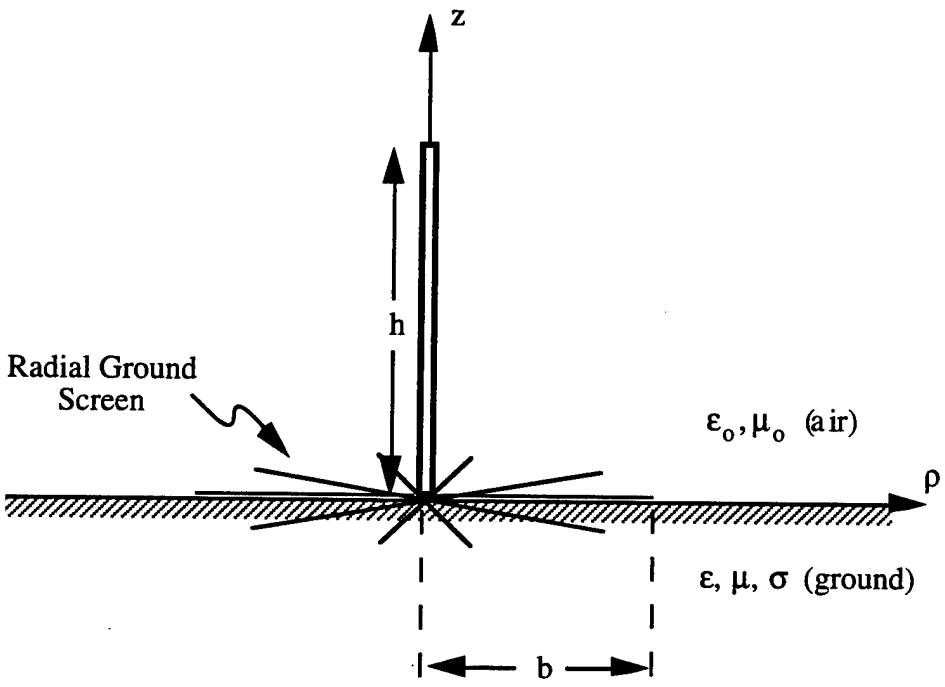


Figure A.2.2: The representation of a vertical monopole with a radial ground screen over an imperfect ground used in this development.

For the region $\rho > b$, the impedance of the ground is just $\eta$, as defined in the beginning of part B of this appendix, but when the ground radials are present ($\rho < b$), the impedance is the parallel combination of the screen impedance, $\eta_e$, and the surface impedance, $\eta$. This is the equivalent impedance term, $\eta_x$:

$$\eta_x (0 < \rho < a) = \frac{\eta\, \eta_e}{\eta + \eta_e}$$

where:

$$\eta_e = \frac{i\, \eta_o d}{\lambda} \ln \frac{d}{2\pi c}$$

$$\text{and} \quad d = \frac{2\pi\rho}{N}$$

d is the spacing between the radial conductors and c is the radius of the wire. This expression is an approximation, originally derived for a wire grid in free space, and is valid if $|\gamma_e d| << 1$, where $\gamma_e$ is the effective propagation constant. This assumes that the wires are close enough electrically to approximate a grid. $\gamma_e$ is defined as:

$$\gamma_e = \left( \frac{\gamma_o^2 + \gamma^2}{2} \right)^{1/2}$$

Returning to the expression for the change in monopole impedance from a perfect to an imperfect ground plane:

$$\Delta Z = - \frac{1}{I_o^2} \int_0^\infty H_\phi^\infty(\rho,0)\, E_\rho(\rho,0)\, 2\pi\rho\, d\rho \qquad \text{(A.2.21a)}$$

we redefine $\Delta Z$ as $\Delta Z_T$, and break it into two parts:

$$\Delta Z_T = \Delta Z + \Delta Z_S$$

where $\Delta Z$ is the change in the input impedance of the antenna due to the influence of the imperfect ground outside the ground screen, and $\Delta Z_S$ is a factor of the imperfect ground screen system. Using the $E\rho$ approximation in (A.2.24):

$$I_o^2 \Delta Z \equiv \eta \int_0^\infty [H_\phi^\infty(\rho,0)]^2 \, 2\pi\rho \, d\rho \qquad \text{(A.2.25)}$$

$$I_o^2 \Delta Z_s \equiv \int_a^b \frac{\eta \, \eta_e}{\eta + \eta_e} [H_\phi^\infty(\rho,0)]^2 \, 2\pi\rho \, d\rho \qquad \text{(A.2.29)}$$

Equation (A.2.25) was developed in part 1 of this appendix and those equations still apply, except that the lower limit of integration is now b, representing the radius of the ground screen. Equation (A.2.29) develops in a similar fashion, except the equivalent impedance term $\eta_x$ is now a function of the radial distance $\rho$, and can no longer be moved outside of the integral. The lower limit a still represents the radius of the conducting base plate. This results in a expression for $\Delta Z_s$ similar to (A.2.27) and (A.2.28) which cannot be solved using the exponential functions:

$$\Delta Z_s = \int_a^b \frac{-\eta_x}{2\pi \sin^2\alpha} \left[ \frac{e^{-j2\beta r}}{\rho^2} \cos^2(\beta h - \alpha) - \frac{2e^{-j\beta(r+\rho)}}{\rho^2} \cos(\beta h - \alpha)\cos\alpha \right.$$
$$- \frac{2jhe^{-j2\beta r}}{r\rho^2} \cos(\beta h - \alpha)\sin(\alpha - \beta h) + \frac{e^{-j2\beta\rho}}{\rho^2} \cos^2\alpha$$
$$\left. + \frac{2jhe^{-j\beta(r+\rho)}}{r\rho^2} \sin(\alpha - \beta h)\cos\alpha - \frac{h^2 e^{-j2\beta r}}{r^2\rho^2} \sin^2(\alpha - \beta h) \right] \rho d\rho$$

$$= \frac{-1}{2\pi \sin^2\alpha} \{ \cos^2(\beta h - \alpha) \int_a^b \eta_x \frac{e^{-j2\beta r}}{\rho} d\rho - 2\cos(\beta h - \alpha)\cos\alpha \int_a^b \eta_x \frac{e^{-j\beta(r+\rho)}}{\rho} d\rho$$
$$- 2jh \cos(\beta h - \alpha) \sin(\alpha - \beta h) \int_a^b \eta_x \frac{e^{-j2\beta r}}{r\rho} d\rho + \cos^2\alpha \int_a^b \eta_x \frac{e^{-j2\beta\rho}}{\rho} d\rho$$
$$+ 2jh \sin(\alpha - \beta h)\cos\alpha \int_a^b \eta_x \frac{e^{-j\beta(r+\rho)}}{r\rho} d\rho - h^2 \sin^2(\alpha - \beta h) \int_a^b \eta_x \frac{e^{-j2\beta r}}{\rho r^2} d\rho \}$$
$$= \Delta Z \qquad \text{(A.2.30)}$$

For the case of no top loading, (h' = 0), $\alpha = \beta h$, and (A.2.30) simplifies to:

$$\Delta Z_s = \frac{-1}{2\pi \sin^2\beta h} \{ \int_a^b \eta_x \frac{e^{-j2\beta r}}{\rho} d\rho - 2\cos\beta h \int_a^b \eta_x \frac{e^{-j\beta(r+\rho)}}{\rho} d\rho$$

$$- \cos^2\beta h \int_a^b \eta_x \frac{e^{-j2\beta\rho}}{\rho} d\rho \} \qquad \text{(A.2.31)}$$

The $\Delta Z$ term in (A.2.25) can be simplified as was done with (A.2.27), by incorporating the exponential function. This is shown below as (A.2.28'), with b representing the extent of the ground screen:

$$\Delta Z = \frac{-\eta}{2\pi \sin^2\beta h} \{ -\frac{1}{2} Ei[-j2\beta(r_o + h)]e^{j2\beta h} - \frac{1}{2} Ei[-j2\beta(r_o - h)]e^{-j2\beta h}$$

$$- 2\cos\beta h \left( - Ei[-j\beta(g+1)h]e^{j\beta h} - Ei[-j\beta(g-1)h]e^{-j\beta h} + Ei[-j\beta hg] \right)$$

$$+ \cos^2\beta h \, (Ei[-j2\beta b]) \} \qquad \text{(A.2.28')}$$

where

$$r_o = (b^2 + h^2)^{1/2} \quad \text{and} \quad g = \frac{b + (b^2 + h^2)^{1/2}}{h}$$

$\Delta Z$ may be simplified further when the height of the monopole is much shorter than the radius of the ground screen, which can often the case for a short vertical whip (with no top loading) in the HF frequency band. Specifically, we limit the height (h) so that $b^2 > 10h^2$, which makes r roughly equivalent to $\rho$, since the limits of the integration are from b to $\infty$. $H_\phi^\infty(\rho,0)$ (for no top loading) becomes:

$$H_\phi^\infty(\rho,0) = \frac{-jI_o}{2\pi \sin\alpha} \left[ \frac{e^{-j\beta\rho}}{\rho} - \frac{e^{-j\beta\rho}}{\rho} \cos\alpha \right] \qquad \text{(A.2.32)}$$

which, when substituted into (A.2.25) results in:

$$\Delta Z = \frac{-\eta}{2\pi \sin^2\beta h} (1 - \cos\alpha)^2 \int_b^\infty \frac{e^{-j2\beta\rho}}{\rho} d\rho \qquad \text{(A.2.33)}$$

$$\Delta Z = \frac{-\eta}{2\pi \sin^2\beta h}(1 - \cos\alpha)^2 \, Ei[-j2\beta a] \qquad \text{(A.2.34)}$$

Solving for $\Delta Z_S$ is much more complicated, because the impedance term, $\eta_x$ , is a function of $\rho$, and because the remaining integrals do not fit into a specific form like the exponential function. The ground/ground screen impedance $\eta_x$ is defined as:

$$\eta_x = \frac{\eta\,\eta_e}{\eta + \eta_e} = \frac{j\eta\eta_o 2\pi\rho \ln\left(\frac{\rho}{NC}\right)}{N\lambda\eta + j\eta_o 2\pi\rho \ln\left(\frac{\rho}{NC}\right)} \qquad \text{(A.2.35)}$$

where N is the number of ground radials, and C is the radial wire thickness. In Section III, the calculated values for $\Delta Z_S$ were found by numerical integration of equation (A.2.31), with (A.2.35) being used for the impedance term.

## Appendix B. Ground Constant Measurements

This section describes the method for determining the ground constants of a prospective antenna test location. The method used was taken from Appendix B of the Hardened Antenna Technology Handbook [10].

The ground constants of an area are found using a monopole probe inserted vertically into the earth. One may derive these constants, the earth's effective conductivity ($\sigma$) and dielectric constant ($\varepsilon$) from measurements taken of the probe's complex input impedance. The monopole probe is treated as a field problem of a capacitor with an unknown dielectric.

The monopole probe is shown in Figure B.1. It comprises an electrically short copper rod, which has a BNC jack attached to one end, and a large (3' X 3') copper plate. The probe is attached to the plate by screwing the BNC jack through a hole in the center of the plate. A nut has been soldered to the plate (to accept the BNC jack) to insure a good connection between the feed cable shield and the plate. Two probe lengths are used, 12" and 18" each with a 3/8" diameter. The plate also has 4 PVC "legs" glued to one side of the plate, which allow the measurement of the monopole probe in air (free space).

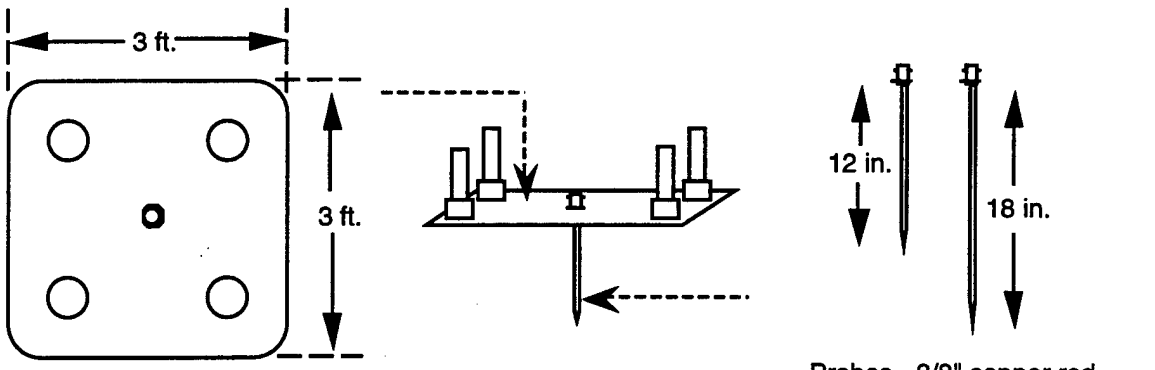


Figure B.1: Monopole Probe Assembly

The test bed is depicted in Figure B.2. An HP 4195A Network Analyzer (hereafter referred to as the analyzer) is connected to the monopole probe through a signal divider (directional bridge) which provides isolation between the reflected (test) and the reference signals. A coaxial cable is used to connect the reflection test set to the probe's BNC jack. Note that the plate is connected through the BNC connector on the probe to ground.

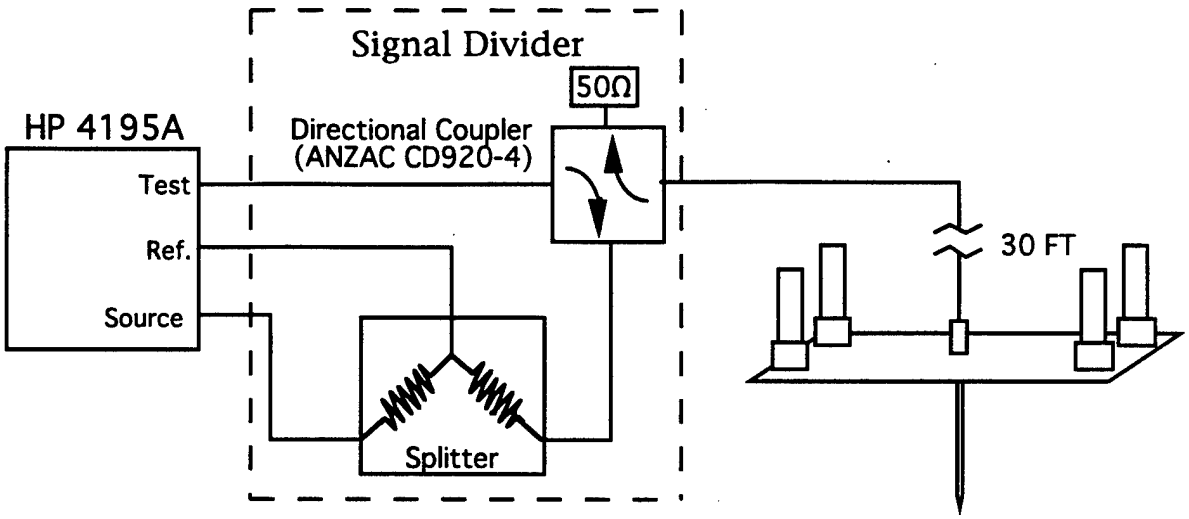


Figure B.2: Test Configuration for Ground Constant Measurements using an HP4195A Network/Spectrum Analyzer with a Monopole Probe

In this set-up, the "Network" configuration of the analyzer is used, and the input impedance of the probe is obtained from the Smith Chart display, using the analyzer's marker to select the particular frequency of interest. In order to compensate for the coaxial cable's length and any losses it might contribute to the impedance measurement of the probe, a one-port full calibration is performed prior to any measurements. Open circuit, short circuit, and 50 ohm load terminations are used to perform the calibration of the analyzer. These terminations are mounted on BNC jacks, and are screwed into the plate in place of the probe during the calibration routine.

The expressions used to calculate the conductivity and dielectric constant of the ground are derived from a general expression for the input admittance of an electrically short linear antenna [11]:

$$Y = j\omega C_o(\varepsilon_r - j\frac{\sigma}{\omega\varepsilon_o}) \qquad (B.1)$$

where:

Y = input admittance of the antenna (monopole probe) in air

$C_o$ = the "static" capacitance of the antenna (according to [10]), which is interpreted to be the capacitance of the probe in air.

Defining $X_o$ as the measured reactance of the probe in air, one makes the following substitutions:

$$X_o \equiv -\frac{1}{\omega C_o}$$

$$\frac{1}{\omega\varepsilon_o} = 60\lambda$$

and (B.1) becomes:

$$Y = -\frac{j\varepsilon_r}{X_o} - \frac{60\lambda\sigma}{X_o} = G + jQ \qquad (B.2)$$

Solving for $\varepsilon_r$ and $\sigma$, and expressing G and Q in terms of R and X, which are the measured resistance and reactance of the probe in the ground, the result is:

$$\sigma = -\frac{X_o}{60\lambda}\left[\frac{R}{R^2 + X^2}\right] \qquad (B.3)$$

$$\varepsilon_r = \frac{X_o X}{R^2 + X^2} \qquad (B.4)$$

where:

R = measured resistance of the monopole probe in the earth

X = measured reactance of the monopole probe in the earth

$X_o$ = measured reactance of the probe in free space (in air)

To obtain the static capacitance $X_o$, the monopole probe reactance is measured with an air dielectric. The monopole probe is placed on its legs with

the probe pointing straight up in the air. The network analyzer is then calibrated, and $X_0$ is measured off the Smith Chart display. One must be careful to calibrate over the entire frequency band being investigated.

For the measurements of the input impedance of the monopole probe in the earth, a reasonably flat section of earth is located, and most of the grass cut away to prevent appreciable air pockets between the plate and the earth from affecting the results. The plate is put in place on the ground, with the PVC legs pointing up. A steel rod (3/8") is driven through the hole in the plate to the depth of the probe to be used. This prevents requiring a lot of force to insert the probe, which could bend the copper rod and/or break off the BNC jack. The rod is removed, and the analyzer is re-calibrated with the plate in this position. The probe is then inserted through the hole into the earth and screwed to the plate. Measurements of the input impedance (R and X) of the probe in the ground are read off the Smith Chart display of the Network Analyzer.

Ground Constant Surveys of Potential Antenna Test Locations

The three sites surveyed for testing the theory set forth in this report were: the Naval Research Laboratory's Waldorf Lower Site Facility in Waldorf, MD, the U.S. Coast Guard Station in Alexandria, VA, and the Naval Electronic Systems Engineering Activity (NESEA) in St. Inigoes, MD. Each site selected contained an area that was flat, relatively large, free of trees and brush, and had no power or sewer lines running underneath which could corrupt the results.

Measurements of the input impedance (R and X) of the probe in the ground and of the static capacitive reactance ($X_0$) were made at 1 MHz intervals from 5 to 20 MHz. The values at each frequency were the result of a visual averaging of a number of swept measurements made by the analyzer. The variation for the readings of Xo at the low end of the frequency band was rather large, but a significant majority of the values have a variation of less than 1%.

Figures B.3 through B.8 are the results of the site surveys, showing the conductivity and dielectric constant of the earth with respect to frequency at each location. Monopole probe measurements were made at four or more positions

within the desired area of operation at each site. Comparing the results, it can be seen that the NESEA site (Figures B.5 and B.8) held the most consistent ground constant values over the entire area surveyed. The Coast Guard site (Figures B.4 and B.7) displayed a great deal of variation from one measurement position within the surveyed area to another. This can possibly be attributed to the high water content in some low-lying sections because of the the poor drainage in the area. Even though measurements at all three sites were done on two different days, there is no great difference from one day to another, except in the case of the NESEA field site, whose dielectric constant was lower (and much more consistent) on the second set of measurements. The weather for each day's measurements hot and dry, with no precipitation during the preceding two days.

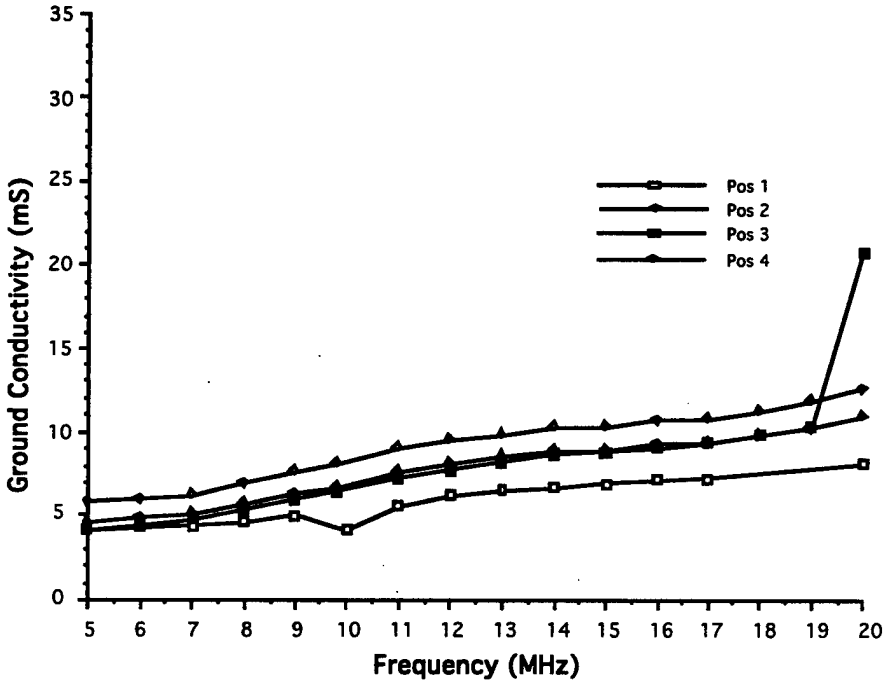


Figure B.3: Ground Conductivity vs. Frequency for NRL Waldorf Lower Site, measured on 6/6/90 (Pos. 1) and 6/13/90 (Pos. 2-4) using a 12" probe.

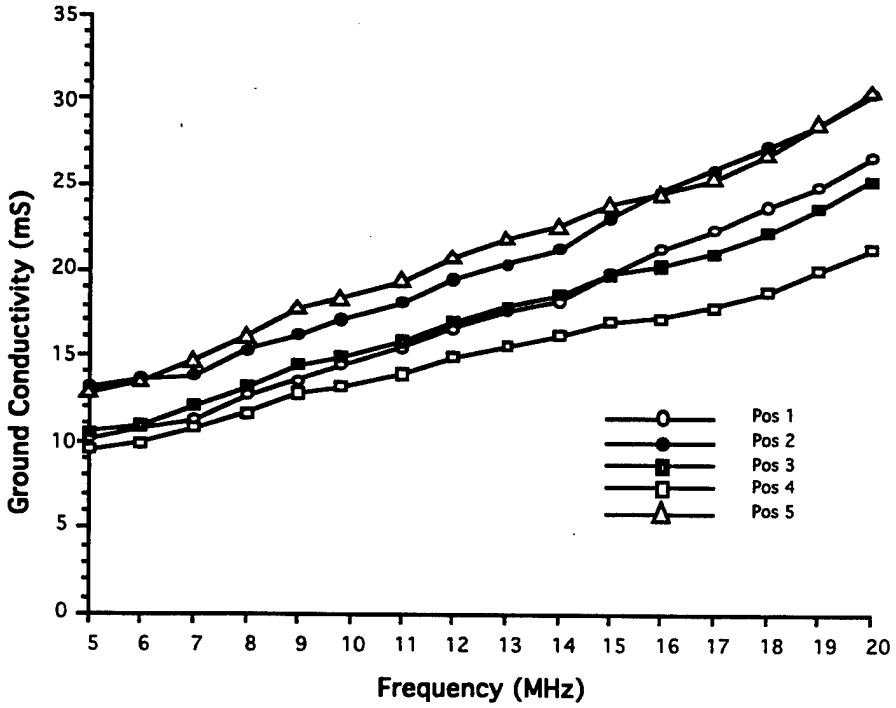


Figure B.4: Ground Conductivity vs. Frequency for Coast Guard Station, measured on 6/13/90 (Pos. 1 & 2) and 6/27/90 (Pos. 3-6) using a 12" probe.

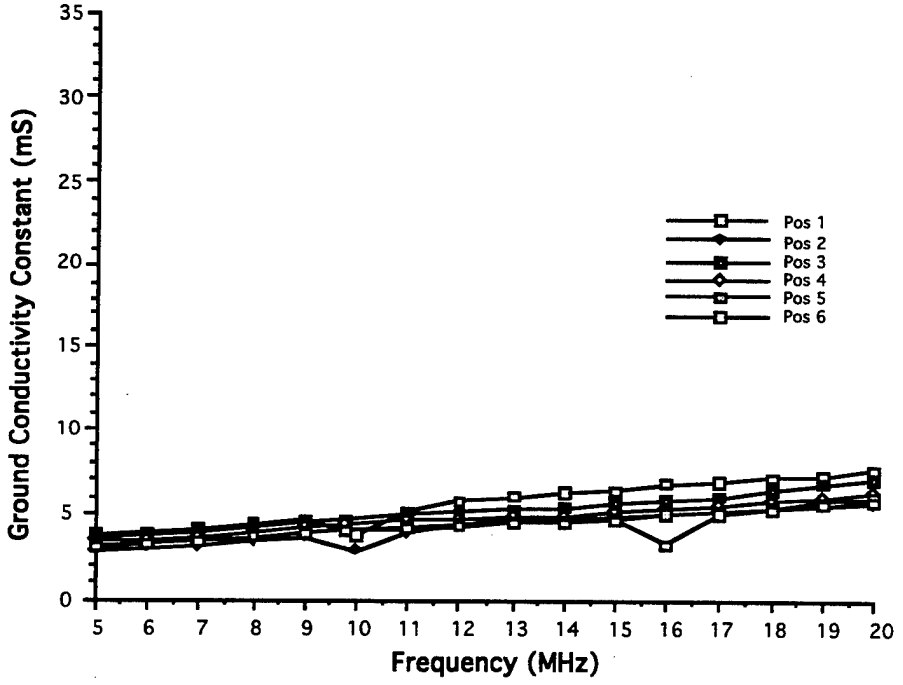


Figure B.5: Ground Conductivity vs. Frequency for NESEA field site, measured on 6/8/90 (Pos. 1 & 2) and 7/3/90 (Pos. 3-6) using a 12" probe.

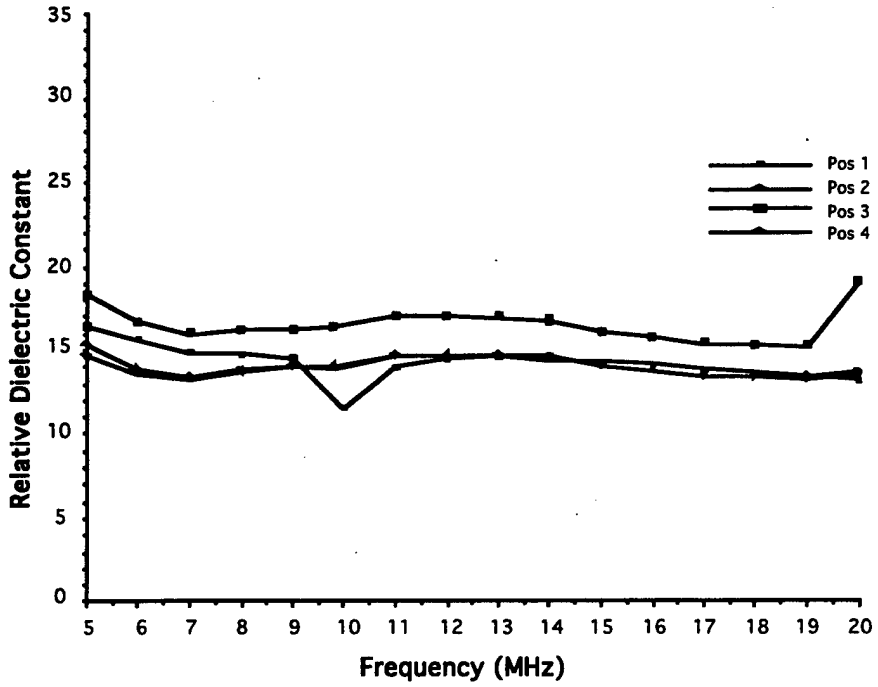


Figure B.6: Relative Dielectric Constant vs. Frequency at NRL Waldorf Lower Site, measured on 6/6/90 (Pos. 1) and 6/13/90 (Pos. 2-4)using a 12" probe.

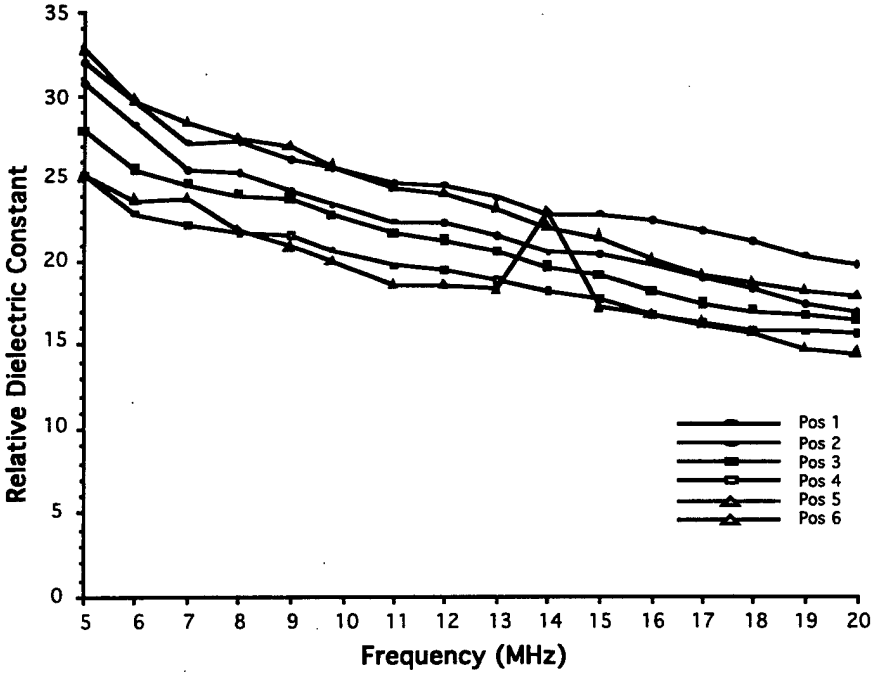


Figure B.7: Relative Dielectric Constant vs. Frequency at Coast Guard Station, measured on 6/13/90 (Pos. 1 & 2) and 6/27/90 (Pos. 3-6)using a 12" probe.

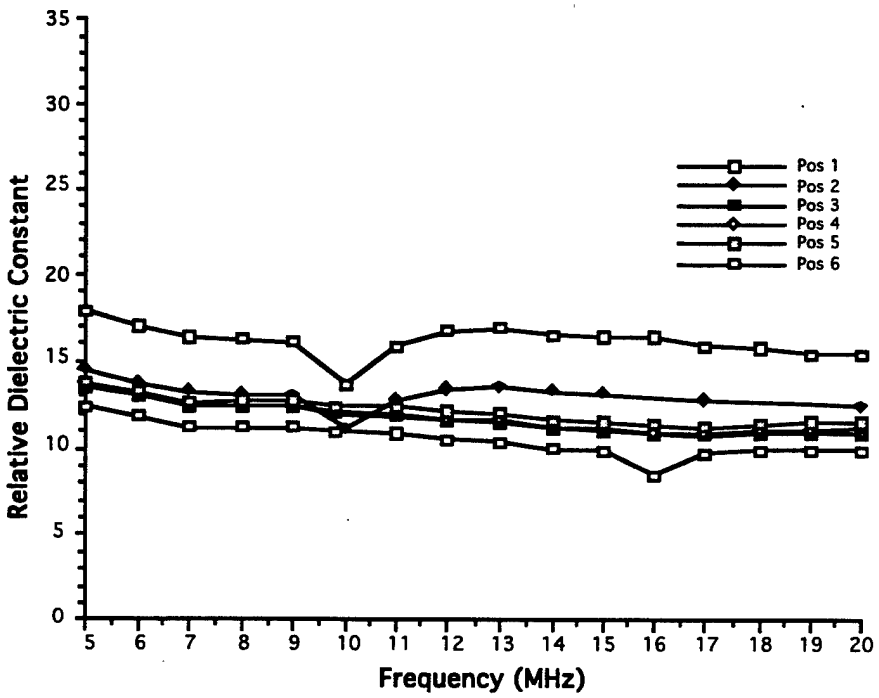


Figure B.8: Relative Dielectric Constant vs. Frequency at NESEA field site, measured on 6/8/90 (Pos. 1 & 2) and 7/3/90 (Pos. 3-6) using a 12" probe

It should be noted that the results of all three sites did not conform to the ground conditions set forth by Wait in [3]. The Waldorf site came the closest to meeting the criteria set forth in equation (2.5) of Section II.